Ph.D. DISSERTATION

Interference Management Algorithms for Multicell MIMO Systems

다중셀 다중안테나 환경을 고려한 간섭제어 기법

BY

DOOHEE KIM

AUGUST 2016

DEPARTMENT OF ELECTRICAL ENGINEERING AND
COMPUTER SCIENCE
COLLEGE OF ENGINEERING
SEOUL NATIONAL UNIVERSITY

Ph.D. DISSERTATION

Interference Management Algorithms for Multicell MIMO Systems

다중셀 다중안테나 환경을 고려한 간섭제어 기법

BY

DOOHEE KIM

AUGUST 2016

DEPARTMENT OF ELECTRICAL ENGINEERING AND
COMPUTER SCIENCE
COLLEGE OF ENGINEERING
SEOUL NATIONAL UNIVERSITY

Interference Management Algorithms for Multicell MIMO Systems

다중셀 다중안테나 환경을 고려한 간섭제어 기법

지도교수 이 광 복
이 논문을 공학박사 학위논문으로 제출함

2016년 8월

서울대학교 대학원

전기 컴퓨터 공학부

김 두 희

김두희의 공학박사 학위 논문을 인준함

2016년 8월

위 원 장: _____
부위원장: _____
위 원: _____
위 원: _____
위 원: _____

Abstract

Intercell interference is one of the most challenging issues limiting the performance of cellular systems, especially when the spectrum is highly reused across cells. In multiple-input multiple-output (MIMO) systems, in particular, it has been reported that, in a multicell environment, the performance of spatial multiplexing is significantly degraded due to intercell interference. In this dissertation, we develop interference management algorithms for multicell MIMO systems.

In the first part of this dissertation, an efficient user selection scheme for the downlink of multiuser MIMO systems is proposed in a multicell environment. In a multicell environment, the intercell interference is one of the most influential factors limiting the performance. Thus, a user selection scheme that considers intercell interference is essential to increase the sum rate. The proposed scheme is based on an interference-aware precoding. It sequentially selects users such that the sum rate is maximized. In particular, we develop a simple incremental metric for the sum rate. The use of the derived metric enables a significant reduction in the computational complexity of the user selection process, as compared to the optimal exhaustive search. Numerical results show that the proposed scheme provides near-optimal performance with substantially reduced complexity.

In the second part of this dissertation, we propose a one-shot (non-iterative) cooperative beamforming scheme for downlink multicell systems. Unlike previous non-iterative beamforming schemes, the proposed cooperative beamforming strives to balance maximizing the desired signal power while minimizing the generated interference power to neighbors by maximizing the network-wide average sum rate. Based on the average sum rate analysis, we derive what we term a global selfishness that steers the egoistic-altruistic balance of the network to maximize average sum rate. The global selfishness enables an autonomous decision on the cooperative beamforming vector in

each cell. The main advantage of our approach is that cooperative beamforming solutions are analytically derived not only for an ideal two-cell network scenario but also for a practical three-sectored cellular network scenario. The simulation results verify that the proposed one-shot cooperative beamforming outperforms other conventional non-iterative schemes especially in interference-limited regions, which implies that it is very effective for performance improvement of edge users.

In the third part of this dissertation, we propose a distributed cell clustering algorithm for coordinated-multi-point (CoMP) system based on message passing algorithm. In 5G networks system, it is expected that a large number of base stations (BSs) serve simultaneously and BSs are deployed in a very high density. Because of this high density systems, the centralized coordination approaches typically lead to high computational burden for practical implementations. Moreover, the sum rate metric are all coupled and it is difficult to determine clusters of BSs. This motivates us to propose a distributed cell clustering scheme based on message passing algorithm. The simulation results verify that the proposed clustering algorithm outperform the conventional distributed algorithm and reduces computational burden compared to centralized clustering algorithms.

keywords: Intercell interference, MIMO, user selection, beamforming, cell clustering
student number: 2011-30217

Contents

Abstract i

Contents iii

List of Tables v

List of Figures vi

1 Introduction 1

1.1 Low Complexity User Selection Algorithm 1

1.2 Non-iterative Beamforming Scheme 2

1.3 Distributed Cell Clustering Algorithm Based on Message Passing . . 5

2 Low Complexity User Selection Algorithm 7

2.1 System Model 7

2.2 Proposed User Selection Algorithm 10

2.2.1 User Selection Criterion 11

2.2.2 User Selection Algorithm 15

2.3 Numerical Results 18

3 Non-iterative Beamforming Scheme 26

3.1 System Model 26

3.2 Proposed One-Shot Cooperative Beamforming 27

3.3 Determination of Global Selfishness λ 31
3.3.1 Ideal Two-cell Network Scenario 31
3.3.2 Practical Three-Sectored Cellular Network Scenario 36
3.3.3 Practical Cellular Network Scenario with N_t antennas 40
3.4 Numerical Results 43

4 Distributed Cell Clustering Algorithm Based on Message Passing 53
4.1 System Model 53
4.2 Message Passing Algorithm 54
4.3 Numerical Results 57

5 Conclusion 62

Abstract (In Korean) 73

Acknowlegement 75

List of Tables

2.1 Comparison of computational complexity. 17

3.1 BSs actions and Corresponding Probabilities 35

3.2 BS_1 actions and Corresponding Probabilities in Three-Sectored Cellular Network 39

3.3 BS_1 actions and Corresponding Probabilities for N_t transmit antennas 42

List of Figures

2.1 $\sum_{j=1}^{n-1} I_j(n-1)$ to $(n-2)I_G(n)$ ratio and $\sum_{j=1}^{n} I_j(n)$ to $nI_G(n)$ ratio vs. SNR, when $K = 10$, $N_t = 4$ and $N_r = 2$. 14

2.2 Average sum rate vs. SNR under the scenario 1, when $K = 10$, $N_t = 4$ and $N_r = 2$. 20

2.3 Average sum rate vs. SNR under the scenario 2, when $K = 10$, $N_t = 4$ and $N_r = 2$. 21

2.4 Average sum rate vs. SNR under the scenario 3, when $K = 10$, $N_t = 4$ and $N_r = 2$. 22

2.5 Average number of selected users vs. SNR under the scenario 1, when $K = 10$, $N_t = 4$ and $N_r = 2$. 23

2.6 Average number of selected users vs. SNR under the scenario 2, when $K = 10$, $N_t = 4$ and $N_r = 2$. 24

2.7 Average number of selected users vs. SNR under the scenario 3, when $K = 10$, $N_t = 4$ and $N_r = 2$. 25

3.1 Framework of the proposed beamforming scheme 30

3.2 Optimal global selfishness λ versus distance of MS from BS 46

3.3 Average sum rate versus SNR in an ideal two-cell network scenario. . 47

3.4 Cumulative distribution of user rate versus user rate in an ideal two-cell network scenario, when SNR=30dB. 48

3.5 Average sum rate versus SNR in a practical three-sectored cellular network scenario. 49
3.6 Cumulative distribution of user rate versus user rate in a practical three-sectored cellular network scenario, when SNR=30dB. 50
3.7 Average sum rate versus SNR in a practical three-sectored cellular network scenario with N_t=4. 51
3.8 Cumulative distribution of user rate versus user rate in a practical three-sectored cellular network scenario with N_t=4, when SNR=30dB. 52

4.1 Average sum rate versus Number of cells in CoMP-JP systems. 58
4.2 Average sum rate versus edge SNR in CoMP-JP systems. 59
4.3 Average sum rate versus Number of cells in CoMP-CS/CB systems. . 60
4.4 Average sum rate versus edge SNR in CoMP-CS/CB systems. 61

Chapter 1

Introduction

Intercell interference is one of the most challenging issues limiting the performance of cellular systems, especially when the spectrum is highly reused across cells. In multiple-input multiple-output (MIMO) systems, in particular, it has been reported that, in a multicell environment, the performance of spatial multiplexing is significantly degraded due to intercell interference [1]. Recently, there have been several works on multicell MIMO that attempt to mitigate the effect of intercell interference. In this dissertation, we develop interference management algorithms for multicell MIMO systems.

1.1 Low Complexity User Selection Algorithm

Most of the works have focused on precoding or beamforming strategies. For instance, centralized precoding schemes were proposed for a case in which the channel state information (CSI) is available at the transmitter [2] and for the case when it is not available [4]. In [5], a distributed precoding scheme was proposed by introducing a new precoding metric known as the signal-to-generated-interference-plus-noise ratio (SGINR). Precoding schemes rely on the condition that the set of users to be served is given. In practice, an appropriate choice of users may have a substantial impact on

the overall system performance in multiuser MIMO scenarios [6-8]. A general framework for user selection was developed in [6] based on convex utility functions. In [7], successive user selection schemes were proposed along with the optimization of transmit beamforming vectors. In [8], various low complexity user selection schemes were proposed. However, these schemes may suffer from severe performance degradation in multicell MIMO systems, as they do not take the intercell interference into account. This motivates us to investigate a user selection scheme applicable to multicell MIMO systems. In this part, we propose a user selection scheme that works jointly with the SGINR-based precoding scheme in [5] for a downlink multicell MIMO system. The SGINR precoding is also known as the signal-to-leakage-and-noise ratio (SLNR) precoding [3], which was discussed in 3GPP LTE-Advanced [9]. The proposed scheme is designed to select users in a successive manner such that the sum rate is maximized. We derive a simple incremental metric, which enables the system to determine whether adding a particular user would increase the sum rate or not. Owing to the derived metric, the proposed scheme requires considerably reduced computational complexity as compared to the optimal exhaustive search over all possible combinations of users. Numerical results will be presented to validate the performance of the proposed user selection scheme under various environments.

1.2 Non-iterative Beamforming Scheme

The sum rate performance is significantly degraded by ICI particularly when a small number of frequency reuse factor is adopted in the network [1]. Thus, there have been seamless efforts to efficiently manage ICI by introducing cooperative beamforming among cells. A well-known example of this effort is the coordinated multi-point (CoMP) technique, which has been rigorously developed for commercial 3rd generation partnership project long term evolution (3GPP-LTE) systems [9, 15]. The main hurdle for the network-wide sum rate maximization is in its mathematical intractabil-

ity. It is very difficult to determine the cooperative beamforming vectors that maximize the desired signal power of one cell while minimizing the generated interference to other cells, as they are all coupled in terms of the sum rate. For the multiple transmit antennas at base station (BS), maximizing the the sum rate is proven to be NP-hard in [16]. Therefore, some alternative approaches have been proposed in the literature [3, 5, 17-29]. The approaches in [17-24] are based on a well-known game theory. The characterizations of achievable rate region and existence of a unique Nash equilibrium have been provided in [17]. Cooperative beamforming vectors are determined by utilizing the two extreme solutions as the basis, i.e., egoistic beamforming and altruistic beamforming. A simple linear-type combination of egoistic beamforming and altruistic beamforming has been shown to achieve Pareto optimality in MISO systems [18]. The extension to a general K-user case has been derived in [19, 20]. For the case when the partial CSI is available at the transmitter, Pareto optimality of MISO system has been shown in [21]. The analysis based on competitive market, called Walrasian market, has studied in [22]. The ICI links and beamforming vectors are considered consumers and goods, respectively. Then, the arbitrator coordinates the transmission strategies for achieving the Pareto optimal Walrasian equilibrium. In [23], a beamforming scheme that uses the generated interference level as a bargaining value has been proposed, where both of instantaneous and statistical CSI are considered. It has been derived the non-strict Pareto boundary of two-user MIMO scenario in [24]. It has solved non-convex problem with rate constraints and extended K-user MIMO system. The second-order cone programming (SOCP) convex problem has been solved for Pareto optimal points in the achievable rate region of MISO systems in [25]. It has been shown to achieve Pareto optimality in M- cells MISO systems. Unfortunately, the aforementioned cooperative beamformings require iterative update procedures to compute cooperative beamforming vectors. Each BS has to recompute new beamforming vectors whenever channel conditions are changed. Thus, this type of approaches typically leads to high computational burden for practical implementations.

For computationally-efficient solutions, the approaches in [3, 5, 26-29] propose non-iterative beamforming schemes. To this end, instead of directly maximizing the sum rate, they aim to define a new metric that considers both desired signal power and generating interference power, maximizing the new metric. In [3] and [5], a new metric is defined as the desired signal power and the generated interference power to neighboring cells plus noise power ratio (SGINR). Then, the cooperative beamforming vector in each cell is individually determined to maximize the SGINR. The SGINR-based cooperative beamforming maximizes the desired signal power and minimizes the generated interference power to neighbors simultaneously, which increases the network-wide sum rate. In an ideal two-cell network scenario, the SGINR-based cooperative beamforming has been shown to achieve near optimal performance that maximizes the network-wide sum rate. For general n-cell cases, the optimality of the SGINR-based cooperative beamforming has not been proved, but the main idea can be generalized by assuming high SINR at all links [5]. In [26-28], similar beamforming schemes have been proposed, which maximize virtual SINR. For an ideal two-cell network scenario, it has been shown that linear-type combination of egoistic beamforming and altruistic beamforming achieves Pareto optimality. In [29], the distributed beamforming scheme that maximizes virtual SINR has been proposed. It has studied reciprocity of the uplink and downlink channels in MISO interference channel to propose the distributed beamforming scheme. The closed-form beamforming solution for K-user MISO interference channel has been derived with some assumptions while conventional virtual SINR beamforming solutions have been derived for two-user scenario. Although the aforementioned non-iterative beamformings in [3, 5, 26-29] maximize SGINR or virtual SINR metric, it is not guaranteed that they can maximize the network-wide sum rate in practical cellular networks. In this paper, we propose a one-shot cooperative beamforming scheme that does not require iterative computations to determine cooperative beamforming vectors. Unlike previous works that focus on maximizing the instantaneous sum rate or virtual SINR, the proposed one-shot cooperative beamform-

ing instead focuses on maximizing the average sum rate. This enables autonomous decision-making in each cell according to the predetermined metric, called global selfishness. The global selfishness implies how much each cell in the network may operate selfishly or altruistically to maximize the network-wide sum rate. This can be computed by analyzing the long-term characteristic of the network, i.e., average sum rate. The main advantage of our approach is that we can derive the cooperative beamforming vectors for a practical three-sectored cellular network scenario as well as an ideal two-cell network scenario, which can be achieved in proposed one-shot beamforming approaches without high SINR assumption unlike the conventional non-iterative beamforming approaches. Based on this, we provide a very useful beamforming strategy for practical cellular systems.

1.3 Distributed Cell Clustering Algorithm Based on Message Passing

The fifth generation (5G) cellular network system is expected that mobile traffics increase 1000 times compared to those of now [31]. Even though there is no global consensus on the definition of 5G network system, high-density small cell network system is widely accepted as one of key techniques in 5G network systems [32, 33]. As base stations (BSs) increase, coordination among BSs becomes the most important technique and it has been widely studied in recent years [10, 15, 34]. This technique is known as coordinated multi-point (CoMP) and it is classified into coordinated scheduling/ coordinated beamforming (CS/CB) and joint processing (JP). CoMP CS/CB system requires channel state information (CSI) but no data sharing among BSs. CoMP JP system requires data sharing as well as CSI among BSs. In this paper, we focus on both CoMP CS/CB system and CoMP JP system. The BSs in coordination systems are connected via backhaul links for exchanging CSI and user data. As the density of BS increases tremendously, to optimize the backhaul overhead, an appropriate cluster-

ing algorithm is essential for efficient CoMP systems. There have been studied some clustering algorithm for CoMP systems [35-43]. A dynamic cell clustering algorithm for multi user distributed antenna system was developed in [35]. It maximizes system capacity with low complexity assuming perfect CSI. In [36], a dynamic interference avoidance scheme was presented for coordination a group of neighboring cells. It minimizes the sum rate performance degradation while also considering cell edge users. A greedy algorithm for dynamic cell clustering was proposed in [37], which maximizes sum rate of MSs considering backhaul overhead of system. In [38], the static clustering algorithm for interference minimization was proposed. It makes two groups considering interference influence, i.e. interior users and edge users and serves with different coordination strategies. The clustering is optimized by maximizing the increase of user rate and by minimizing interference power in [39]. An iterative clustering algorithm for heterogeneous networks was proposed in [40]. It uses sparse optimization techniques to select a subset of base station and design precoding vectors. A dynamic cell clustering algorithm for multi-stream transmission was developed in [41], where the clusters change over time adapting the channel conditions. In [42], a dynamic cell clustering algorithm for maximizing the coordination gain in the uplink CoMP system. It improves the average user rate with reducing computational complexity. Unfortunately, the aforementioned clustering algorithms works in centralized manners which requires exhaustive information sharing and bring substantial computational complexity. Considering high density CoMP systems, a clustering algorithm is essential for reducing information sharing and computational complexity. A clustering algorithm where each cluster using only local information between neighboring BSs was proposed in [43]. It reduces backhaul overhead and computational complexity by using affinity propagation [44]. However, it was proposed heuristic algorithm and limited in CoMP JP systems. In this paper, we propose a distributed cell clustering algorithm for CoMP system based on message passing algorithm. Our proposed clustering algorithm is applicable CoMP CS/CB systems as well as CoMP JP systems.

Chapter 2

Low Complexity User Selection Algorithm

2.1 System Model

We consider the downlink of a cellular system comprised of L cells or sectors and K users per cell or sector. Each base station (BS) and each mobile station (MS) are assumed to be equipped with N_t transmit antennas and N_r receive antennas, respectively. The L cells or sectors are grouped into a cluster of $L = 3$. Each BS is assumed to serve only the users in its own cell using the interference-aware precoding scheme in [5]. The received signal vector $\mathbf{y}_i^{(k)}$ at the k^{th} MS of the i^{th} cell can be expressed as

$$\begin{aligned} \mathbf{y}_i^{(k)} &= \sqrt{\rho_i^{(k)}}\mathbf{H}_{i,i}^{(k)}\mathbf{W}_i^{(k)}\mathbf{x}_i^{(k)} + \sum_{j=1,j\neq k}^{K}\sqrt{\rho_i^{(k)}}\mathbf{H}_{i,i}^{(k)}\mathbf{W}_i^{(j)}\mathbf{x}_i^{(j)} \\ &+ \sum_{m=1,m\neq i}^{L}\sum_{j=1}^{K}\sqrt{\eta_{i,m}^{(k)}}\mathbf{H}_{i,m}^{(k)}\mathbf{W}_m^{(j)}\mathbf{x}_m^{(j)} + \mathbf{n}_i^{(k)}, \end{aligned} \tag{2.1}$$

where $\mathbf{x}_i^{(k)}$ denotes the transmit symbol destined for the k^{th} MS in the i^{th} cell, $\mathbf{W}_i^{(k)}$ is the corresponding precoding matrix, $\mathbf{H}_{i,m}^{(k)}$ is an $N_r \times N_t$ channel matrix between the BS in the m^{th} cell and the k^{th} MS in the i^{th} cell. The entries of the channel matrix $\mathbf{H}_{i,m}^{(k)}$ are assumed to follow independent and identically distributed (i.i.d) complex Gaussian distribution with zero mean and unit variance. $\mathbf{n}_i^{(k)}$ denotes the additive white Gaussian noise (AWGN), $\rho_i^{(k)}$ denotes the signal-to-noise ratio (SNR) of the k^{th} MS in the i^{th} cell, and $\eta_{i,m}^{(k)}$ denotes the interference-to-noise ratio (INR) for the interference

that the BS in the m^{th} cell causes at the k^{th} MS in the i^{th} cell. The transmit symbols and noise are assumed to be normalized to have unit power. We assume that every BS has the same transmit power P, and that each BS allocates equal transmit power to the selected users in the corresponding cell; when M users are selected from a BS, each user is allocated to the power of P/M. The first term in (4.1) corresponds to desired signal, and the second and third terms represent the intracell interference and intercell interference, respectively, within a cluster. Note that both the intracell interference and intercell interference constitute the intracluster interference, and the intercluster interference is not considered.

The cell coordination model considered in this paper falls into the category of coordinated scheduling/coordinated beamforming (CS/CB) in the context of LTE-Advanced. In a CS/CB, BSs need to share only the CSI through a coordinator, and each BS serves users in its own cell [10]. We assume that the precoding matrix $\mathbf{W}_i^{(k)}$ for each MS in (4.1) is formed based on the SGINR criterion [5]. It was shown that the SGINR-based beamforming improves the sum rate in a multicell environment. Specifically, the SGINR covariance matrix $\mathbf{K}_{\mathbf{GI}_i}^{(k)}$ at the k^{th} MS in the i^{th} cell is defined as

$$\mathbf{K}_{\mathbf{GI}_i}^{(k)} = \rho_i^{(k)} \left(\mathbf{I}_{N_t} + \mathbf{G}_i^{(k)^H} \mathbf{G}_i^{(k)} \right)^{-1} \left(\mathbf{H}_{i,i}^{(k)^H} \mathbf{H}_{i,i}^{(k)} \right), \tag{2.2}$$

where

$$\mathbf{G}_i^{(k)} \equiv \left[\left(\mathbf{H}_{\mathbf{G}1,i}^{(k)} \right)^T \cdots \left(\mathbf{H}_{\mathbf{G}i,i}^{(k)} \right)^T \cdots \left(\mathbf{H}_{\mathbf{G}L,i}^{(k)} \right)^T \right]^T \tag{2.3}$$

denotes a composite matrix containing both the intercell interference channels and the intracell interference channel that the k^{th} MS in the i^{th} cell may cause to other users, $(\cdot)^H$ denotes the conjugate transpose, and $(\cdot)^T$ denotes the transpose of a matrix. Each submatrix of $\mathbf{G}_i^{(k)}$ is defined as

$$\mathbf{H}_{\mathbf{G}j,i}^{(k)} = \begin{cases} \left[\sqrt{\rho_i^{(1)}} \mathbf{H}_{i,i}^{(1)} \cdots \sqrt{\rho_i^{(k+1)}} \mathbf{H}_{i,i}^{(k+1)} \cdots \sqrt{\rho_i^{(K)}} \mathbf{H}_{i,i}^{(K)} \right], & i = j \\ \left[\sqrt{\eta_{j,i}^{(1)}} \mathbf{H}_{j,i}^{(1)} \cdots \sqrt{\eta_{j,i}^{(K)}} \mathbf{H}_{j,i}^{(K)} \right], & i \neq j. \end{cases} \tag{2.4}$$

To construct a beamforming matrix $\mathbf{W}_i^{(k)}$, we express $\mathbf{K}_{\mathbf{GI}_i}^{(k)}$ in (2.2) using the eigenvalue decomposition as

$$\mathbf{K}_{\mathbf{GI}_i}^{(k)} = \mathbf{V}_{\mathbf{GI}_i}^{(k)} \mathbf{D}_{\mathbf{GI}_i}^{(k)} \mathbf{V}_{\mathbf{GI}_i}^{(k)H}, \tag{2.5}$$

where $\mathbf{D}_{\mathbf{GI}_i}^{(k)}$ and $\mathbf{V}_{\mathbf{GI}_i}^{(k)}$ denote the diagonal matrix composed of eigenvalues and unit-norm eigenvector matrix of $\mathbf{K}_{\mathbf{GI}_i}^{(k)}$, respectively. Then, $\mathbf{V}_{\mathbf{GI}_i}^{(k)}$ corresponds to a beamforming matrix: $\mathbf{W}_i^{(k)} = \mathbf{V}_{\mathbf{GI}_i}^{(k)}$ [5]. Thus, the precoding and user selection require centralized processing, i.e., CSI sharing among cells. Each BS in a cluster collects information on both the desired channel and interference channels for each MS. For the k^{th} MS in the i^{th} cell, for example, $\mathbf{H}_{i,i}^{(K)}$ corresponds to the desired channel matrix, and $\mathbf{H}_{\mathbf{G}}{}_{j,i}^{(k)}, j \neq i$ correspond to interference channel matrices. It is assumed that the MS perfectly estimates both the desired and interference channels and feeds them back to the BS without error. The BS transports the CSI to a cluster coordinator, which then performs the beamforming and user selection, and notifies the results back to the associated BSs.

Assuming that each MS employs the maximum likelihood (ML) detection, the achievable rate $R_i^{(k)}$ of the k^{th} MS in the i^{th} cell can be computed as

$$R_i^{(k)} = \log_2 \det \left(\mathbf{I}_{N_r} + \mathbf{\Lambda}_i^{(k)} \right), \tag{2.6}$$

where $\mathbf{\Lambda}_i^{(k)}$ denotes a matrix associated with the received signal-to-interference-plus-noise ratio (SINR) of the k^{th} MS in the i^{th} cell [2]. It is given as

$$\mathbf{\Lambda}_i^{(k)} = \rho_i^{(k)} \left(\mathbf{H}_{i,i}^{(k)} \mathbf{W}_i^{(k)} \right) \left(\mathbf{\Gamma}_i^{(k)} \right)^{-1} \left(\mathbf{H}_{i,i}^{(k)} \mathbf{W}_i^{(k)} \right)^H, \tag{2.7}$$

where $\mathbf{\Gamma}_i^{(k)}$ represents the noise plus interference power:

$$\begin{aligned} \mathbf{\Gamma}_i^{(k)} &= \mathbf{I}_{N_r} + \sum_{j=1, j\neq k}^{K} \rho_i^{(j)} \left(\mathbf{H}_{i,i}^{(j)} \mathbf{W}_i^{(j)} \right) \left(\mathbf{H}_{i,i}^{(j)} \mathbf{W}_i^{(j)} \right)^H \\ &+ \sum_{m=1, m\neq i}^{L} \sum_{j=1}^{K} \eta_{i,m}^{(j)} \left(\mathbf{H}_{i,m}^{(j)} \mathbf{W}_m^{(j)} \right) \left(\mathbf{H}_{i,m}^{(j)} \mathbf{W}_m^{(j)} \right)^H. \end{aligned} \tag{2.8}$$

On the right hand side of (2.8), the first term is due to the AWGN, and the second and third terms represent the intracell interference and intercell interference, respectively.

Using (4.3), the corresponding sum rate $\mathcal{R}_{sum}$ for all MS's in the cluster of L cells is given by

$$\mathcal{R}_{sum} = \sum_{i=1}^{L} \sum_{k=1}^{K} R_i^{(k)}. \tag{2.9}$$

2.2 Proposed User Selection Algorithm

In this section, we propose a user selection scheme that works in a multicell environment. Because the achievable rate in (4.3) is affected by the intercell interference as well as by the intracell interference, it may not be optimal in terms of the sum rate that each BS serves all K users at the same time. Therefore, the proper selection of simultaneously served users will be important to optimize the overall performance. The greedy user selection algorithm in [11] is known to provide near optimal sum rate performance in a single cell scenario. However, the greedy algorithm does not consider the intercell interference, which may lead to inevitable performance degradation in a multicell environment. In [2], it was shown that the optimal solution approaches a single stream transmission scheme as the intercell interference becomes strong.

We propose a user selection algorithm that maximizes the sum rate in (2.9) in a multicell environment. Let $U_i \equiv \{(i,1),(i,2),\cdots,(i,K)\}$ represent the set of all users in the i^{th} cell, and let $\mathcal{S}_i^*$ be the set of selected users in the i^{th} cell. The user selection problem can then be formulated as

$$\mathcal{S}^* = \underset{\mathcal{S}_i \subset U_i,\ i=1,2,\cdots,L}{\arg\max} \sum_{i=1}^{L} \sum_{k \in \mathcal{S}_i} R_i^{(k)}, \tag{2.10}$$

where $\mathcal{S}^* \equiv \mathcal{S}_1^* \cup \mathcal{S}_2^* \cup \cdots \cup \mathcal{S}_L^*$ denotes the resulting set of all selected users. The solution of (2.10) will require an exhaustive search over all possible combinations of users, which may cause high computational complexity. As a more practical solution to (2.10), we propose a suboptimal successive user selection scheme based on the SGINR precoding. We explain the details of the user selection criterion and the selection algorithm in the following subsections.

2.2.1 User Selection Criterion

Given that the proposed user selection scheme successively adds users to the set of its served users one-by-one, we need to develop a criterion to determine whether to add a user or not at each step. Suppose that $(n-1)$ $(n \geq 2)$ users are already selected and they are represented by a set of the user indices, $\mathcal{S}^*(n-1) \equiv \{(i_1, k_1), \cdots, (i_{n-1}, k_{n-1})\}$, where i_j and k_j represent the BS index and MS index of the j^{th} selected user, respectively. Let $\Delta R(n)$ be the increment in the sum rate when user (i_n, k_n) is added to the set $\mathcal{S}^*(n-1)$ to form $\mathcal{S}^*(n) = \mathcal{S}^*(n-1) \cup \{(i_n, k_n)\}$. Then, $\Delta R(n)$ can be expressed as

$$\begin{aligned} \Delta R(n) &= \sum_{(i,k)\in\mathcal{S}^*(n)} \log_2 \det\left(\mathbf{I}_{N_r} + \mathbf{\Lambda}_i^{(k)}(n)\right) \\ &- \sum_{(i,k)\in\mathcal{S}^*(n-1)} \log_2 \det\left(\mathbf{I}_{N_r} + \mathbf{\Lambda}_i^{(k)}(n-1)\right), \end{aligned} \tag{2.11}$$

where $\sum_{(i,k)\in\mathcal{S}^*(n)}$ indicates that the sum is taken over n (i,k) pairs associated with the user indices in $\mathcal{S}^*(n)$ when the n users in $\mathcal{S}^*(n)$ are simultaneously served. We approximate $\Delta R(n)$ in (2.11) as

$$\Delta R(n) \approx \sum_{(i,k)\in\mathcal{S}^*(n)} \log_2 \det\left(\mathbf{\Lambda}_i^{(k)}(n)\right) - \sum_{(i,k)\in\mathcal{S}^*(n-1)} \log_2 \det\left(\mathbf{\Lambda}_i^{(k)}(n-1)\right), \tag{2.12}$$

which follows from the assumption that the selected users have high SINR[1] [5].

Then, $\Delta R(n)$ in (2.12) can be rewritten and upper bounded as

$$\Delta R(n) \approx \log_2 \left[\frac{\left(\frac{S_1(n)}{I_1(n)}\right) \cdots \left(\frac{S_n(n)}{I_n(n)}\right)}{\left(\frac{S_1(n-1)}{I_1(n-1)}\right) \cdots \left(\frac{S_{n-1}(n-1)}{I_{n-1}(n-1)}\right)} \right] \leq \log_2 \left[\left(\prod_{\ell=1}^{n-1} \frac{I_\ell(n-1)}{I_\ell(n)} \right) \frac{S_n(n)}{I_n(n)} \right], \tag{2.13}$$

where $S_\ell(n)$ and $I_\ell(n)$, respectively, represent the received signal component and the noise plus interference component for the ℓ^{th} selected user, when the n users in $\mathcal{S}^*(n)$

[1] It should be noted that the approximation is used just to simplify the incremental metric for user selection. The high SINR assumption should not restrict the derived metric to being used only at high SINR. In Section 2.3, we will consider a situation in which all the MSs are distributed over the cell edge area where the SINR is generally low.

are served simultaneously. These can be expressed as

$$\begin{aligned} S_\ell(n) &= \det\left(\rho_{i_\ell}^{(k_\ell)}(\mathbf{H}_{i_\ell,i_\ell}^{(k_\ell)}\mathbf{W}_{i_\ell}^{(k_\ell)})(\mathbf{H}_{i_\ell,i_\ell}^{(k_\ell)}\mathbf{W}_{i_\ell}^{(k_\ell)})^H\right), \\ I_\ell(n) &= \det\left(\mathbf{R}_{\mathbf{I}\ell}(n)\right), \end{aligned} \tag{2.14}$$

where $\mathbf{R}_{\mathbf{I}\ell}(n)$ denotes the noise plus received interference matrix, when the n users in $\mathcal{S}^*(n)$ are served. The notation i_ℓ indicates the ℓ^{th} selected user associated to the BS in the i^{th} cell. The matrix $\mathbf{R}_{\mathbf{I}\ell}(n)$ can be expressed as

$$\begin{aligned} \mathbf{R}_{\mathbf{I}\ell}(n) &= \mathbf{I}_{N_r} + \sum_{(i,k),i=i_\ell} \rho_{i_\ell}^{(k_\ell)} \left(\mathbf{H}_{i_\ell,i_\ell}^{(k_\ell)}\mathbf{W}_i^{(k)}\right)\left(\mathbf{H}_{i_\ell,i_\ell}^{(k_\ell)}\mathbf{W}_i^{(k)}\right)^H \\ &+ \sum_{(i,k),i\neq i_\ell} \eta_{i_\ell,i}^{(k_\ell)} \left(\mathbf{H}_{i_\ell,i}^{(k_\ell)}\mathbf{W}_i^{(k)}\right)\left(\mathbf{H}_{i_\ell,i}^{(k_\ell)}\mathbf{W}_i^{(k)}\right)^H, \end{aligned} \tag{2.15}$$

and $\mathbf{W}_i^{(k)}$ denotes the SGINR precoding matrix when n users in $\mathcal{S}^*(n)$ are simultaneously served. Note that the inequality in (2.13) is due to $\prod_{\ell=1}^{n-1} S_\ell(n) \leq \prod_{\ell=1}^{n-1} S_\ell(n-1)$, which follows from the term-by-term inequalities $S_\ell(n) \leq S_\ell(n-1), \ell = 1, 2, \cdots, n-1$. The term-by-term inequalities are valid due to the following reasons. First, when the n^{th} user is added up, $n-1$ users that are already selected should be allocated to transmit power equal to or less than the value for the case when only $n-1$ users are selected, owing to the assumption of transmit power in Section 2.1. Moreover, when the n^{th} user is added, it generates additional interference to the other $n-1$ users, and thus will decrease the received signal power of each MS.

We further assume $\sum_{\ell=1}^{n-1} I_\ell(n-1) \leq (n-2)I_G(n)$ and $\sum_{\ell=1}^{n} I_\ell(n) \leq nI_G(n)$, where $I_G(n)$ denotes the noise plus generated interference component of the n^{th} selected user:

$$\begin{aligned} I_G(n) &= \det\left(\mathbf{G}_{\mathbf{I}n}(n)\right), \\ \mathbf{G}_{\mathbf{I}n}(n) &= \mathbf{I}_{N_r} + \sum_{(i,k),i=i_n} \rho_i^{(k)} \left(\mathbf{H}_{i,i}^{(k)}\mathbf{W}_{i_n}^{(k_n)}\right)\left(\mathbf{H}_{i,i}^{(k)}\mathbf{W}_{i_n}^{(k_n)}\right)^H \\ &+ \sum_{(i,k),i\neq i_n} \eta_{i,i_j}^{(k)} \left(\mathbf{H}_{i,i_n}^{(k)}\mathbf{W}_{i_n}^{(k_n)}\right)\left(\mathbf{H}_{i,i_n}^{(k)}\mathbf{W}_{i_n}^{(k_n)}\right)^H. \end{aligned} \tag{2.16}$$

The assumptions are reasonable in that the generated interference power of the last selected user will be greater than those of the previously selected users, because all users

have similar received signal power and the user selection is performed sequentially based on the SGINR. Figure 2.1 verifies that the $\sum_{\ell=1}^{n-1} I_\ell(n-1)$ to $(n-2)I_G(n)$ ratio and the $\sum_{\ell=1}^{n} I_\ell(n)$ to $nI_G(n)$ ratio are less than unity in the typical SNR range. Using the inequality of the arithmetic and geometric means with the two assumptions, we can derive the following two inequalities:

$$\begin{aligned} \prod_{\ell=1}^{n-1} I_\ell(n-1) &\leq \left(\tfrac{1}{n-1}\sum_{\ell=1}^{n-1}\left(I_\ell(n-1)\right)\right)^{n-1} \leq \left(\tfrac{n-2}{n-1}I_G(n)\right)^{n-1}, \\ \prod_{\ell=1}^{n} I_\ell(n) &\leq \left(\tfrac{1}{n}\sum_{\ell=1}^{n}\left(I_\ell(n)\right)\right)^{n} \leq \left(I_G(n)\right)^{n}. \end{aligned} \tag{2.17}$$

Using the upper bounds in (2.13) and (2.17), we approximate $\Delta R(n)$ as

$$\Delta R(n) \approx \log_2 \left[\frac{\left(\frac{n-2}{n-1}I_G(n)\right)^{n-1} S_n(n)}{\left(I_G(n)\right)^n}\right], \quad n \geq 2. \tag{2.18}$$

Accordingly, we define the metric $\Delta r(n)$ as

$$\Delta r(n) \equiv 2^{\Delta R(n)} = \left(\frac{n-2}{n-1}\right)^{n-1} \frac{S_n(n)}{I_G(n)}, \quad n \geq 2. \tag{2.19}$$

It is observed that the metric $\Delta r(n)$ in (2.19) corresponds to a weighted SGINR. For a specific case of $n = 1$, it is obvious that selecting the user associated with the maximum SNR is optimal in term of the sum rate. Hence, we define $\Delta r(1) \equiv \det\left(\rho_i^{(k)}(\mathbf{H}_{i,i}^{(k)})(\mathbf{H}_{i,i}^{(k)})^H\right)$. Note that $\Delta r(n)$, which is the proposed criterion for user selection, depends on the transmit beamforming vector for $n \geq 2$.

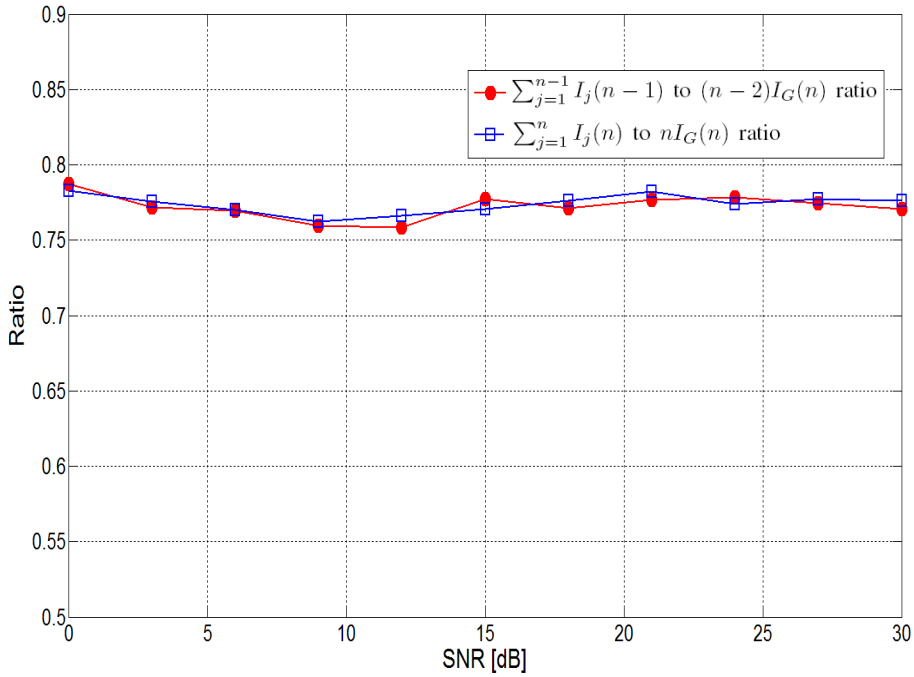

Figure 2.1: $\sum_{j=1}^{n-1} I_j(n-1)$ to $(n-2)I_G(n)$ ratio and $\sum_{j=1}^{n} I_j(n)$ to $nI_G(n)$ ratio vs. SNR, when $K = 10$, $N_t = 4$ and $N_r = 2$.

2.2.2 User Selection Algorithm

In this section, we propose a user selection algorithm with the objective of sum rate maximization. In the previous subsection, we have defined $\Delta r(n)$ as a criterion for user selection. In order to maximize the sum rate, BSs select users by using $\Delta r(n)$. If $\Delta r(n)$ is larger than 1, which means that sum rate is increased by selecting the n^{th} user, the n^{th} user is selected and added to $\mathcal{S}^*$. Otherwise, the n^{th} user are not selected and the user selection procedure is terminated. Specifically, the proposed algorithm is described as the following three steps.

- Step 1) Initialize as $\mathcal{S}^*(0) = \phi$ and $n = 1$.

- Step 2) Compute $\Delta r_i^{(k)}(n)$, and find (i_n, k_n) such that
$$(i_n, k_n) = \underset{(i,k)\in(U_1\cdots\cup U_L)-\mathcal{S}^*(n-1)}{\arg\max} \Delta r_i^{(k)}(n),$$
where $\Delta r_i^{(k)}(n)$ denotes the $\Delta r(n)$ corresponding to the k^{th} MS in the i^{th} cell.

- Step 3) If $\Delta r_{i_n}^{(k_n)}(n) > 1$, then set $\mathcal{S}^*(n) = \mathcal{S}^*(n-1) \cup \{i_n, k_n\}$, $n = n + 1$ and go back to Step 2); otherwise, terminate the algorithm.

In Step 1), the set of selected users $\mathcal{S}^*(0)$ is initialized as an empty set. In Step 2), a user associated with the maximum $\Delta r(n)$ is chosen from among the users not in $\mathcal{S}^*(n-1)$. In Step 3), if the value of $\Delta r(n)$ is greater than 1, the corresponding user index is added to $\mathcal{S}^*(n)$ and the algorithm is repeated from Step 2). Otherwise, the algorithm terminates and the final set of selected user is determined as $\mathcal{S}^*(n-1)$.

It should be noted that the proposed algorithm requires much lower computational complexity than the exhaustive search. Since the computational complexity of a user selection scheme mainly comes from computation of the precoding matrices, we measure the computational complexity in terms of the required number of computing precoding matrices. The proposed scheme requires at most $L(N_t/N_r)$ iterations and one user is selected at each iteration. Correspondingly, the complexity of the proposed

scheme can be found to be $\sum_{i=1}^{N_t/N_r} (LK - i + 1)$. The exhaustive search needs to compute precoding matrices for all possible sets of users, and the max-user exhaustive search also needs to compute precoding matrices for all possible sets of (N_t/N_r) users. Based on these computations, the overall computational complexity of each scheme is tabulated in Table2.1. It can be seen that the complexity of the proposed scheme is much lower than that of the exhaustive search and max-user exhaustive search. When $L = 3$, $K = 10$, $N_t = 4$, and $N_r = 2$, for instance, the overall computational complexity of the proposed scheme is 165, whereas that of the exhaustive search and max-user exhaustive search is 4,397,880 and 3,562,650, respectively.

Table 2.1: Comparison of computational complexity.

	Proposed scheme	**Exhaustive search**	**Max-user exhaustive**
Complexity*	$\sum_{i=1}^{L(N_t/N_r)} (LK - i + 1)$	$\sum_{i=1}^{L(N_t/N_r)} (i \times {}_{LK}C_i)$	$L(N_t/N_r) \cdot {}_{LK}C_{L(N_t/N_r)}$

*The complexity is measured in terms of the required number of computing precoding matrices.

2.3 Numerical Results

In this section, we evaluate the performance of the proposed user selection scheme. We consider a cluster composed of three cells ($L = 3$), each of which corresponds to a sector of sectored cells. The average channel gain between the BS in the i^{th} cell and the k^{th} MS in the cell is defined as $E\left[\left\|\mathbf{H}_{i,i}^{(k)}\right\|^2\right] = \rho_0 \left(d_{i,k}/d_r\right)^{-\alpha}$, where $d_{i,k}$ denotes the distance between a BS in the i^{th} cell and k^{th} MS, and ρ_0 denotes the SNR at a distance d_r from the base station. The reference distance d_r can be regarded as the cell radius. The values of d_r, ρ_0 and the pathloss exponent α are set to 500m, 8dB, and 3.7, respectively. The performance of the proposed scheme is compared with that of the exhaustive search, the max-user exhaustive search, and the single cell greedy selection in [11]. In addition, a joint processing scheme based on the dirty paper coding (DPC) is used to provide an upper bound as in [12, 13]. However, it should be noted that the joint processing requires sharing of data as well as the CSI among cells in each cluster, while the other schemes require sharing of only the CSI. In the exhaustive search, all the BSs in the cluster selects optimal user set that maximizes sum rate. The max-user exhaustive search is a modified version of the optimal exhaustive search; in which each BS always selects a set of N_t/N_r users that maximizes the sum rate differently from the exhaustive search. The max-user exhaustive search can be considered as a form of coordinated greedy selection. In the single cell greedy selection, each BS independently selects users associated with the maximum SINR without considering the intercell interference.

We consider three scenarios of user distribution to evaluate the performance of the coordinated user selection schemes. Scenario 1 corresponds to the case in which all users are located in cell edge areas in between $0.9R$ and R, scenario 2 corresponds to the case where all the users are located in between $0.5R$ and R, where R denotes the cell radius, and scenario 3 corresponds to the case where all the users are located uniformly over the entire cell. The reason why we consider scenarios 1 and 2 is that users around cell center can be served separately by each cell without coordination,

since the impact of the intercell interference will be limited. Figures 2.2 - 2.4 depict the achievable sum rate and Figures 2.5 - 2.7 illustrate the average number of selected users vs. SNR under these three scenarios, respectively, when $K = 10$, $N_t = 4$, and $N_r = 2$. From Figures 2.2 - 2.4, the proposed scheme is shown to significantly outperform the single cell greedy selection and the max-user exhaustive search. Moreover, the performance degradation as compared to the exhaustive search seems not that much considering the substantial reduction in the complexity. For instance, when $L = 3$, $K = 10$, $N_t = 4$, and $N_r = 2$, the proposed scheme achieves about 94% of the sum rate of the exhaustive search, while the reduction in computational complexity amounts to about 26,600 fold. As expected, the performance of the joint processing is better than the other schemes at the cost of the backhaul overhead for data sharing among cells. From Figures 2.5 - 2.7, it can be observed that not all the degrees of freedoms at the BS are used to transmit as many streams as possible. This suggests that using all the degrees of freedoms is not always optimal for sum rate. Some degrees of freedoms need to be used for interference mitigation, in such a way that the average sum rate is maximized. As an extreme case, when the SNR is sufficiently high, the proposed solution is shown to approach the single-user scheme, as discussed in [2]. The results in Figure 2.4 also verify that the performance gain of the proposed scheme is substantial even when users are uniformly distributed throughout the cell.

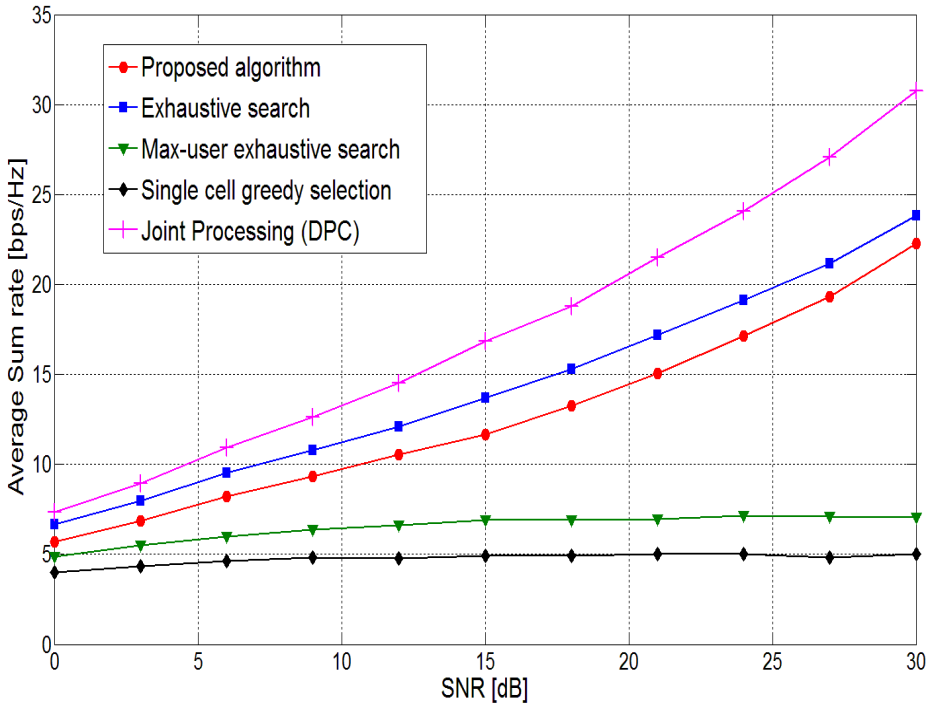

Figure 2.2: Average sum rate vs. SNR under the scenario 1, when $K = 10$, $N_t = 4$ and $N_r = 2$.

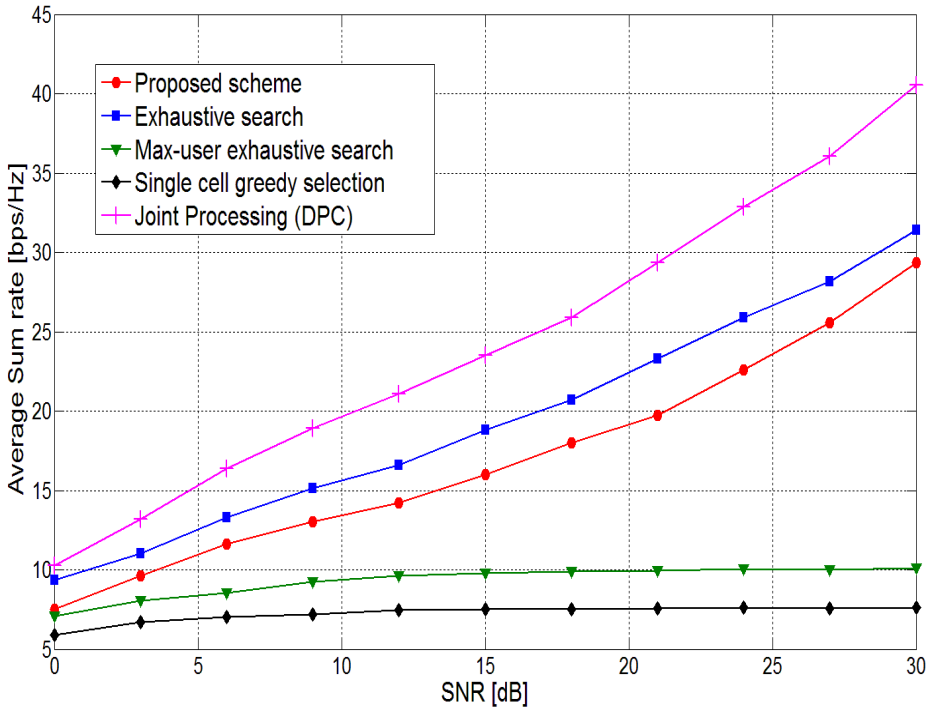

Figure 2.3: Average sum rate vs. SNR under the scenario 2, when $K = 10$, $N_t = 4$ and $N_r = 2$.

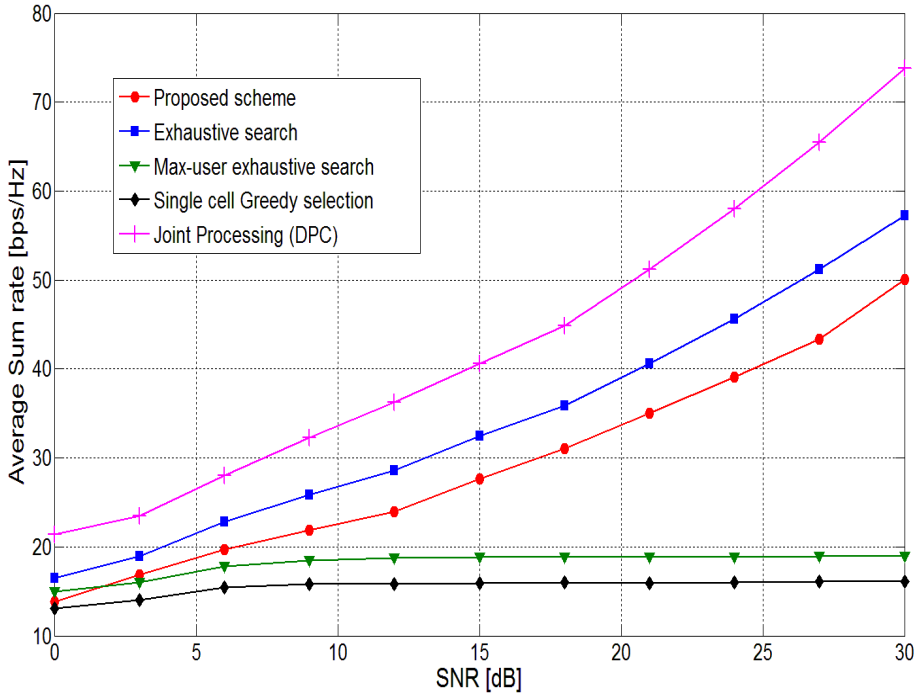

Figure 2.4: Average sum rate vs. SNR under the scenario 3, when $K = 10$, $N_t = 4$ and $N_r = 2$.

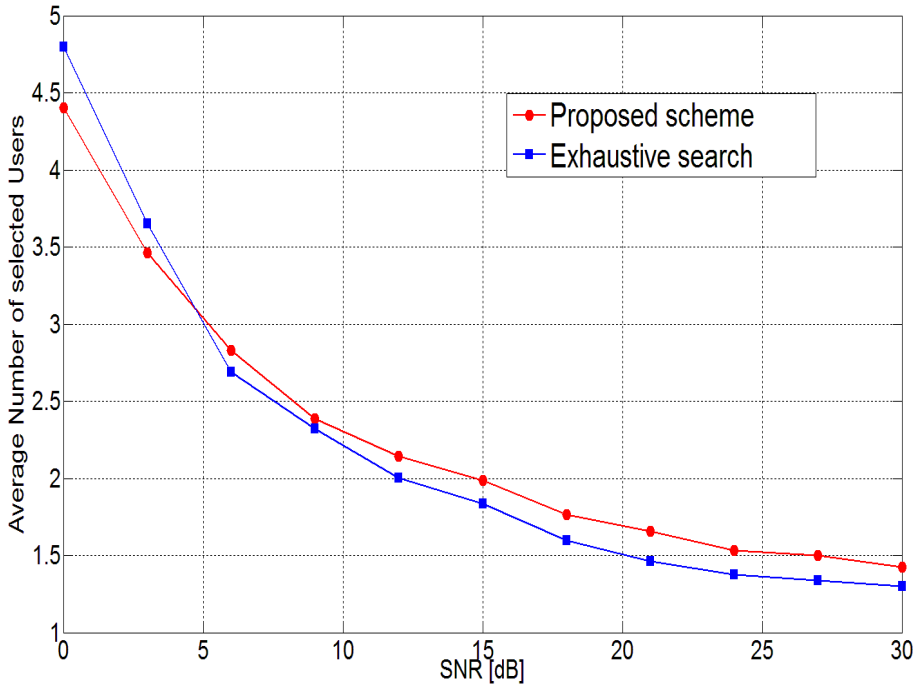

Figure 2.5: Average number of selected users vs. SNR under the scenario 1, when $K = 10$, $N_t = 4$ and $N_r = 2$.

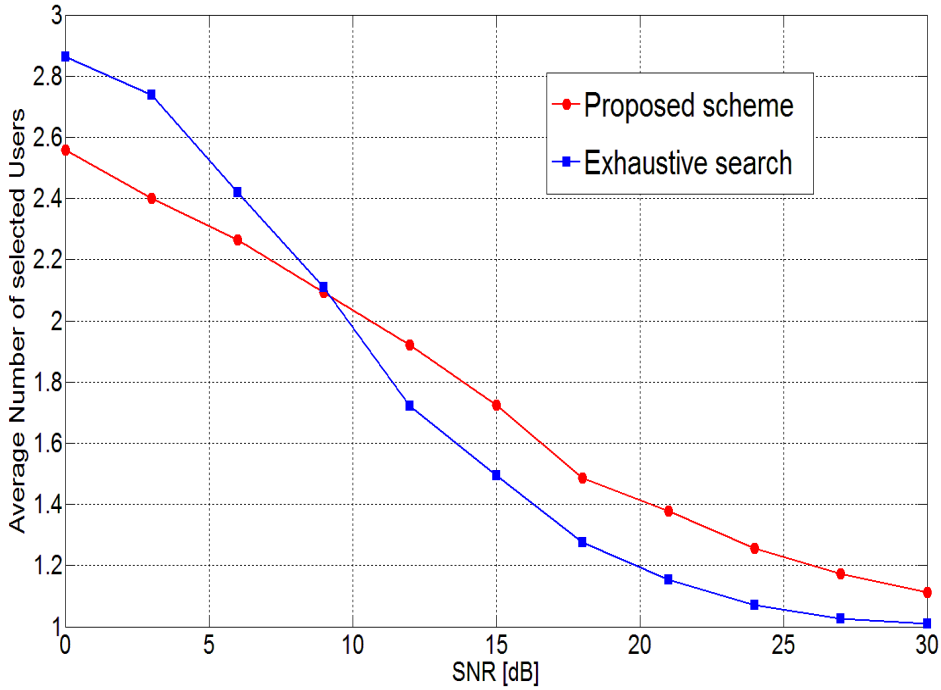

Figure 2.6: Average number of selected users vs. SNR under the scenario 2, when $K = 10$, $N_t = 4$ and $N_r = 2$.

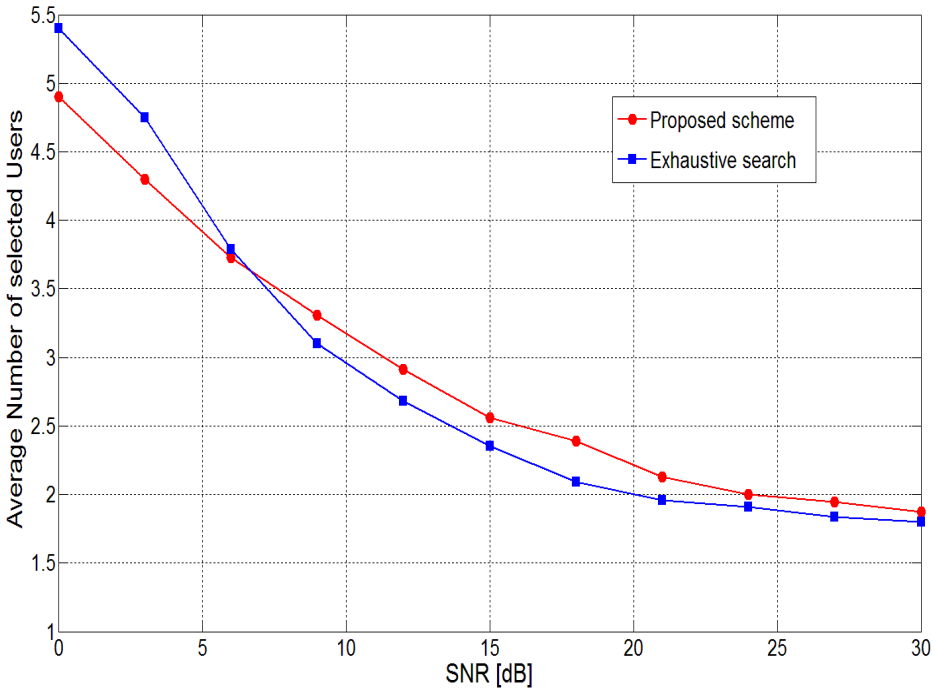

Figure 2.7: Average number of selected users vs. SNR under the scenario 3, when $K = 10$, $N_t = 4$ and $N_r = 2$.

Chapter 3

Non-iterative Beamforming Scheme

3.1 System Model

We consider a downlink cellular system comprised of M cells. We assume that single mobile station (MS) in each cell is already selected to be served by scheduler. Each BS is equipped with N_t antennas and the MS has a single antenna. The received signal vector $\mathbf{y}_i$ at the MS in the i^{th} cell can be expressed as

$$\mathbf{y}_i = \sqrt{\rho_i}\mathbf{h}_{ii}\mathbf{w}_i\mathbf{x}_i + \sum_{j=1,j\neq i}^{M} \sqrt{\rho_{ji}}\mathbf{h}_{ji}\mathbf{w}_j\mathbf{x}_j + \mathbf{n}_i, \tag{3.1}$$

where $\mathbf{h}_{ji}$ denotes $1 \times N_t$ channel vector between BS in the j^{th} cell and the MS in the i^{th} cell, $\mathbf{w}_i$ denotes $N_t \times 1$ corresponding beamforming vector at the BS in the i^{th} cell, and it is normalized, i.e., $||\mathbf{w}_i||^2 = 1$. $\mathbf{x}_i$ is the signal transmitted from the i^{th} BS to the i^{th} MS. We assume that the elements of $\mathbf{h}_{ji}$ follow independent and identically distributed complex Gaussian distribution with zero mean and unit variance. In addition, $\mathbf{n}_i$ denotes the additive white Gaussian noise (AWGN) at the i^{th} MS with unit variance, ρ_i denotes the average signal-to-noise ratio (SNR) of the MS in the i^{th} cell, and ρ_{ji} is the average interference-to-noise ratio (INR) for the interference that the BS in the j^{th} cell causes to the MS in the i^{th} cell. The received SINR γ_i of the MS in the

i^{th} cell can be computed from (4.1) as

$$\gamma_i = \frac{\rho_i |\mathbf{h}_{ii}\mathbf{w}_i|^2}{1 + \sum\limits_{j=1, j\neq i}^{M} \rho_{ji} |\mathbf{h}_{ji}\mathbf{w}_j|^2}. \tag{3.2}$$

From (4.2), the network-wide sum rate of all cells $\mathcal{R}$ is given as

$$\mathcal{R} = \sum_{i=1}^{M} \log_2 (1 + \gamma_i). \tag{3.3}$$

3.2 Proposed One-Shot Cooperative Beamforming

In this section, we propose a new one-shot cooperative beamforming that operates in a non-iterative manner. The proposed one-shot cooperative beamforming focuses on maximizing the average sum rate. At the cost of averaging out local interactions of the network, we can achieve the network-wide balance between egoism and altruism for cooperative beamforming vector computations. The derived metric, global selfishness, significantly relieves the computational burden by providing a simple decision rule for computing cooperative vectors in each cell. In Figure 3.1, we illustrate the detailed procedure of the proposed beamforming scheme. The proposed beamforming scheme consists of two stages, i.e. global optimization stage and distributed optimization stage. A network coordinator in the global optimization stage gathers long-term channel statistics, i.e. SNR and INR are influenced by location of users and transmit power. On the basis of gathered long-term information, the network coordinator determines the optimal value of global selfishness $\lambda^\star$ that maximizes network-wide sum rate. The network-wide sum rate analysis and the detailed derivation of the decision metric will be described in the following section. Then, the network coordinator broadcasts the optimal value of global selfishness $\lambda^\star$ to all BSs. Each BS in the distributed optimization stage gathers short-term CSI and determines precoding vectors by checking the CSI of interference channel with $\lambda^\star$. Then, each BS transmits signals for users with determined precoding vector. During normal downlink transmission, each BS

operates in a distributed optimization stage. At the end of long-term duty cycle, the updating process of global selfishness is initiated in the global optimization stage.

The global selfishness can be interpreted as the amount that each cell can behave selfishly or altruistically to maximize the network-wide sum rate. The optimal value of the global selfishness $\lambda^\star$ is precomputed and shared as a network policy. Once BSs share the optimal value of global selfishness $\lambda^\star$ that is computed by the network coordinator in the global optimization stage, each BS simply computes precoding vector with $\lambda^\star$ in the distributed optimization stage and the required CSI for beamforming is same as distributed beamforming schemes. Since the updating process of global selfishness requires long-term duty cycle, amount of sharing information among BSs becomes minimal as in distributed beamforming schemes. Regarding computational complexity, the proposed scheme can reduce computational burden compared to centralized beamforming schemes. The computational burden in the global optimization stage has less influence on complexity of whole system since the updating process of global selfishness requires long-term duty cycle. In this sense, the proposed beamforming scheme works in semi-distributed manner. Each cell behaves either selfishly or altruistically according to the statistical channel conditions and given $\lambda^\star$. Specifically, the i^{th} cell determines whether its interference links to neighboring cells are dominant or not by checking the channel gains of the interference links with $\lambda^\star$ as $\Phi_i = \left\{ j | \, \|\mathbf{h}_{ij}\|^2 \geq \lambda^\star \right\}$, where Φ_i denotes the set of dominant interference links of the i^{th} cell. The beamforming vector is then computed to nullify the dominant interference links as

$$|\mathbf{h}_{ij}\mathbf{w}_i|^2 = 0, \quad \forall j \in \Phi_i. \tag{3.4}$$

When $\lambda^\star$ is small, the entire network enters an altruistic mood where each cell tends to determine its cooperative beamforming vector that nullifies interference power to its neighboring cells. In the limit of $\lambda^\star \to 0$, the proposed beamforming nullifies all the interference links, and becomes equivalent to the well-known ZF beamforming. The opposite is true for large $\lambda^\star$, and the proposed beamforming becomes equivalent to the

MRT beamforming in the limit of $\lambda^{\star} \to \infty$.

Note that the proposed beamforming scheme can reduce computation complexity by using global selfishness. The computation complexity of beamforming scheme mainly comes from computations of precoding vectors. The proposed beamforming scheme requires only a single matrix inversion of precoding vector, however, the conventional iterative beamforming schemes requires dozens of computations for precoding vectors. Therefore, compared to conventional iterative beamforming schemes, the proposed beamforming scheme can significantly reduce the computational burden.

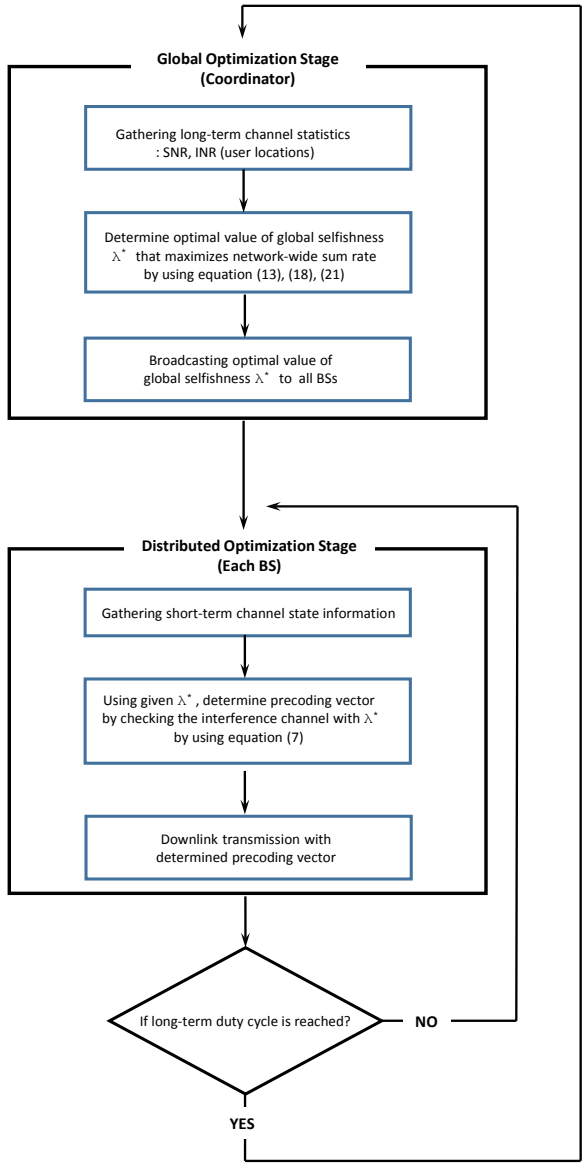

Figure 3.1: Framework of the proposed beamforming scheme

3.3 Determination of Global Selfishness λ

In this section, we first describe how to determine the optimal value of global selfishness for an ideal two-cell network scenario. Then, we expend our results to a practical three-sectored cellular network scenario. For easy understanding, we provide derivations assuming two transmit antennas in the following Sec. 3.3.1 and 3.3.2. However, our results are not limited to the case. We expand our scheme to arbitrary N_t transmit antennas scenario in Sec. 3.3.3.

3.3.1 Ideal Two-cell Network Scenario

We describe how to determine the optimal value of global selfishness for an ideal two-cell network scenario. There exist four possible cases depending on whether each BS acts in an egoistic or an altruistic way. Those cases and corresponding probabilities are tabulated in Table 3.1, where ψ is defined as $\psi = \mathbb{P}\left(||\mathbf{h}_{ji}||^2 > \lambda\right)$ and $\bar{\psi} = 1-\psi$. Case 1 implies that all BSs operate selfishly where no BS nullifies interference links. In the case 2 and case 3, one BS nullifies its generated interference link, and the other BS operates selfishly. Case 4 implies that all BSs nullify the generated interference link and all MSs whose received interference link are nullified. Then, for further derivations, we define random variable $\Gamma_i^{(e_i,a_i)}$ indicates SINR of the MS in the i^{th} cell where the i^{th} BS nullifies e_i generated interference links to neighboring cells and a_i received interference links of the MS in the i^{th} cell are nullified by the neighboring BSs. Then, we can expressed $\Gamma_i^{(e_i,a_i)}$ by using [30, Lemma 2] as

$$\Gamma_i^{(e_i,a_i)} = 1 + \frac{\rho_i \chi^2_{2(N_t-e_i)}}{1 + \sum\limits_{j\in\Omega_i} \rho_{ji}\chi_2^2}, \tag{3.5}$$

where Ω_i denotes the set of neighboring cells of i^{th} cell except the number of a_i BSs that nullify the generated interference links to the MS in the i^{th} cell. χ_n^2 denotes the Chi-square distribution random variable with n degrees of freedom. Then, considering the four possible cases and given ψ, we derive $\mathcal{R}(\psi)$ the sum rate function of ψ from

(4.3) using (3.5) as

$$\begin{aligned}\mathcal{R}(\psi) =&\bar{\psi}^2\log_2\left(\Gamma_1^{(0,0)}\Gamma_2^{(0,0)}\right)+\psi^2\log_2\left(\Gamma_1^{(1,1)}\Gamma_2^{(1,1)}\right)\\&+\psi\bar{\psi}\left(\log_2\left(\Gamma_1^{(0,1)}\Gamma_2^{(1,0)}\right)+\log_2\left(\Gamma_1^{(1,0)}\Gamma_2^{(0,1)}\right)\right)\\=&\bar{\psi}^2\log_2\left(\Pi_{(0,0)}^{(0,0)}\right)+\psi^2\log_2\left(\Pi_{(1,1)}^{(1,1)}\right)+\psi\bar{\psi}\log_2\left(\Pi_{(1,0)}^{(0,1)}\Pi_{(0,1)}^{(1,0)}\right),\end{aligned}\tag{3.6}$$

where $\Pi_{(a_1,a_2)}^{(e_1,e_2)}$ represents the product of $\Gamma_i^{(e_i,a_i)}$ is defined as

$$\Pi_{(a_1,a_2,..,a_n)}^{(e_1,e_2,..,e_n)}=\Gamma_1^{(e_1,a_1)}\Gamma_2^{(e_2,a_2)}\times\cdot\cdot\times\Gamma_n^{(e_n,a_n)}.\tag{3.7}$$

For sum rate analysis, we derive the expected sum rate and its upper bound is denoted as $\mathcal{R}^{\mathrm{U}}(\psi)$. Then, it can be expressed as

$$\begin{aligned}\mathbb{E}[\mathcal{R}(\psi)] =&\bar{\psi}^2\mathbb{E}\left[\log_2\left(\Pi_{(0,0)}^{(0,0)}\right)\right]+\psi^2\mathbb{E}\left[\log_2\left(\Pi_{(1,1)}^{(1,1)}\right)\right]+\psi\bar{\psi}\mathbb{E}\left[\log_2\left(\Pi_{(1,0)}^{(0,1)}\Pi_{(0,1)}^{(1,0)}\right)\right]\\\leq&\bar{\psi}^2\log_2\left(\mathbb{E}\left[\Pi_{(0,0)}^{(0,0)}\right]\right)+\psi^2\log_2\left(\mathbb{E}\left[\Pi_{(1,1)}^{(1,1)}\right]\right)\\&+\psi\bar{\psi}\log_2\left(\left(\mathbb{E}\left[\Pi_{(1,0)}^{(0,1)}\right]\right)\left(\mathbb{E}\left[\Pi_{(0,1)}^{(1,0)}\right]\right)\right)\\\equiv&\mathcal{R}^{\mathrm{U}}(\psi),\end{aligned}\tag{3.8}$$

where the inequality follows from Jensen's inequality. $\Gamma_1^{(e_1,a_1)}$ and $\Gamma_2^{(e_2,a_2)}$ are independent, then the expectation of $\Pi_{(a_1,a_2)}^{(e_1,e_2)}$ can be expressed as

$$\bar{\Pi}_{(a_1,a_2)}^{(e_1,e_2)}=\mathbb{E}\left[\Pi_{(a_1,a_2)}^{(e_1,e_2)}\right]=\mathbb{E}\left[\Gamma_1^{(e_1,a_1)}\right]\mathbb{E}\left[\Gamma_2^{(e_2,a_2)}\right].\tag{3.9}$$

We derive the details of $\mathbb{E}[\Gamma_i^{(e_i,a_i)}]$ of (3.9) in Appendix A. Then, $\mathcal{R}^{\mathrm{U}}(\psi)$ can be expressed as

$$\begin{aligned}\mathcal{R}^{\mathrm{U}}(\psi) =&\bar{\psi}^2\log_2\left(\bar{\Pi}_{(0,0)}^{(0,0)}\right)+\psi^2\log_2\left(\bar{\Pi}_{(1,1)}^{(1,1)}\right)+\psi\bar{\psi}\log_2\left(\bar{\Pi}_{(1,0)}^{(0,1)}\bar{\Pi}_{(0,1)}^{(1,0)}\right)\\=&a\psi^2+b\psi+c,\end{aligned}$$

and

$$a\equiv\log_2\left(\frac{\bar{\Pi}_{(0,0)}^{(0,0)}\bar{\Pi}_{(1,1)}^{(1,1)}}{\bar{\Pi}_{(1,0)}^{(0,1)}\bar{\Pi}_{(0,1)}^{(1,0)}}\right),\quad b\equiv\log_2\left(\frac{\bar{\Pi}_{(1,0)}^{(0,1)}\bar{\Pi}_{(0,1)}^{(1,0)}}{\left(\bar{\Pi}_{(0,0)}^{(0,0)}\right)^2}\right),\quad c\equiv\log_2\left(\bar{\Pi}_{(0,0)}^{(0,0)}\right).\tag{3.10}$$

Using the closed-form expression of $\mathcal{R}^{\mathrm{U}}(\psi)$ in (3.10), we determine the optimal value $\psi^{\star}$ that maximizes $\mathcal{R}^{\mathrm{U}}(\psi)$ as

$$\psi^{\star} = \arg\max_{\psi} \mathcal{R}^{\mathrm{U}}(\psi). \tag{3.11}$$

Note that $\mathcal{R}^{\mathrm{U}}(\psi)$ is a quadratic function of ψ. We first consider that $\mathcal{R}^{\mathrm{U}}(\psi)$ is a concave function ($a < 0$). The point of pole ψ^D becomes the optimal point of ψ if ψ^D is located in [0,1]. If ψ^D is less than 0 or greater than 1, the optimal value of ψ is 0 or 1, respectively. Next, we consider that $\mathcal{R}^{\mathrm{U}}(\psi)$ is a convex function ($a > 0$). Either 0 or 1, i.e., whichever is closer to ψ^D, becomes the optimal $\psi^{\star}$. In short, $\psi^{\star}$ is determined as

$$\begin{aligned}
&\text{(i) } a < 0, \qquad \psi^{\star} = \begin{cases} 0 & \text{if} \quad \psi^D < 0 \\ \psi^D & \text{if} \quad 0 \le \psi^D \le 1 \\ 1 & \text{if} \quad 1 < \psi^D \end{cases} \\
&\text{(ii) } a > 0, \qquad \psi^{\star} = \begin{cases} 0 & \text{if} \quad \left|\psi^D\right| > \left|\psi^D - 1\right| \\ 1 & \text{if} \quad \left|\psi^D\right| \le \left|\psi^D - 1\right|, \end{cases} \\
&\text{where} \qquad \psi^D = -b/2a, \ \text{ s.t. } \left[\frac{\partial \mathcal{R}^{\mathrm{U}}(\psi)}{\partial \psi}\right]_{\psi=\psi^D} = 0.
\end{aligned} \tag{3.12}$$

Furthermore, we can determine the optimal value of the global selfishness $\lambda^{\star}$ from $\psi^{\star}$, since $||\mathbf{h}_{ji}||^2$ has a Gamma(N_t,2) distribution and there is one-to-one correspondence between ψ and λ. The value of $\lambda^{\star}$ is computed from $\psi^{\star}$ as

$$\lambda^{\star} = F^{-1}(1 - \psi^{\star}; N_t, 2), \tag{3.13}$$

where $F(x; N_t, 2)$ denotes the cumulative distribution function (cdf) of Gamma(N_t,2) and $F^{-1}(\cdot)$ denotes the inverse function of cdf. Thus, $\lambda^{\star}$ can be uniquely determined with $\psi^{\star}$.

The principal advantage of the proposed one-shot cooperative beamforming is that it requires much less computational complexity; it only requires a simple comparison of a channel with the given $\lambda^{\star}$. Since the computational complexity of scheme mainly comes from computations of the precoding vectors, we compare the computational complexity in terms of the required number of computations for precoding vectors.

The proposed scheme requires only a single computation of precoding vector, however, the conventional iterative beamforming schemes in [17 - 24] require dozens of computations for precoding vectors, for example, the iterative scheme in [18] requires about 30 repeats of precoding vector computations.

Table 3.1: BSs actions and Corresponding Probabilities

Case #	BS_1 action	BS_2 action	Probability
Case 1	Egoistic	Egoistic	$\bar{\psi}^2$
Case 2	Egoistic	Altruistic	$\bar{\psi}\psi$
Case 3	Altruistic	Egoistic	$\bar{\psi}\psi$
Case 4	Altruistic	Altruistic	ψ^2

3.3.2 Practical Three-Sectored Cellular Network Scenario

For practical applications of the proposed one-shot beamforming scheme, we extend our results to a three-sectored cellular network scenario, which is the most typical structure in recent wireless systems. Note that the conventional approaches to non-iterative beamforming in [3, 5, 26 - 29] fail to provide analytic beamforming solution for $M > 2$ cases, without assuming high SINR, which is obviously not valid for cell edge regions. Moreover, the conventional approaches maximize sum of the V-SINR metric instead of sum rate metric and the gap between sum of V-SINR metric and sum rate metric becomes larger in general $M > 2$ cases. Whereas our approach easily enables this extension because the proposed scheme focuses on average sum rate and all the SINR regions, which can be analyzed as follows. For easy understanding, we provide derivations assuming two transmit antennas in the followings and BS_i nullifies the most dominant one interference link of Φ_i. However, our results are not limited to the case. In this scenario, each BS has three different actions. Taking BS_1 as an example, those cases and corresponding probabilities are tabulated in Table 3.2. Since interference channels are independent, BS_1 has same probability for each altruistic action for MS_2 and MS_3. Therefore, there are a total of $3^3 = 27$ different cases for three-sectored networks. Then, $\mathcal{R}(\psi)$ from (4.3) can be expressed as

$$
\begin{aligned}
&\mathcal{R}(\psi) \\
=&\left(\frac{1}{2}\psi\right)^3 \log_2\left(\Pi_{(1,1,1)}^{(1,1,1)}\Pi_{(1,1,1)}^{(1,1,1)}\Pi_{(2,1,0)}^{(1,1,1)}\Pi_{(2,0,1)}^{(1,1,1)}\Pi_{(1,2,0)}^{(1,1,1)}\Pi_{(1,0,2)}^{(1,1,1)}\Pi_{(0,2,1)}^{(1,1,1)}\Pi_{(0,1,2)}^{(1,1,1)}\right) \\
&+\left(\frac{1}{2}\psi\right)^2 \bar{\psi}\log_2\left(\Pi_{(1,1,0)}^{(1,1,0)}\Pi_{(0,1,1)}^{(1,1,0)}\Pi_{(1,0,1)}^{(1,1,0)}\Pi_{(0,0,2)}^{(1,1,0)}\Pi_{(1,1,0)}^{(1,0,1)}\Pi_{(0,1,1)}^{(1,0,1)}\times\right. \\
&\qquad\left.\Pi_{(1,0,1)}^{(1,0,1)}\Pi_{(0,2,0)}^{(1,0,1)}\Pi_{(1,1,0)}^{(0,1,1)}\Pi_{(1,0,1)}^{(0,1,1)}\Pi_{(0,1,1)}^{(0,1,1)}\Pi_{(2,0,0)}^{(0,1,1)}\right) \\
&+\left(\frac{1}{2}\psi\right)\bar{\psi}^2\log_2\left(\Pi_{(0,1,0)}^{(1,0,0)}\Pi_{(0,0,1)}^{(1,0,0)}\Pi_{(1,0,0)}^{(0,1,0)}\Pi_{(0,0,1)}^{(0,1,0)}\Pi_{(1,0,0)}^{(0,0,1)}\Pi_{(0,1,0)}^{(0,0,1)}\right) \\
&+\bar{\psi}^3\log_2\left(\Pi_{(0,0,0)}^{(0,0,0)}\right). \qquad (3.14)
\end{aligned}
$$

Then, we derive the expected sum rate and its upper bound for sum rate analysis in the same way of (3.8). The expectation of $\Gamma_i^{(e_i,a_i)}$ for three-sectored cellular scenario is derived in Appendix B. Since $\Gamma_1^{(e_1,a_1)}$, $\Gamma_2^{(e_2,a_2)}$ and $\Gamma_3^{(e_3,a_3)}$ are independent, we can easily calculate $\bar{\Pi}_{(a_1,a_2,a_3)}^{(e_1,e_2,e_3)}$. Therefore, $\mathcal{R}^{\mathrm{U}}(\psi)$ can be expressed as

$$
\begin{aligned}
&\mathbb{E}[\mathcal{R}(\psi)] \\
\leq&\left(\frac{1}{2}\psi\right)^3 \log_2\left(\bar{\Pi}_{(1,1,1)}^{(1,1,1)}\bar{\Pi}_{(1,1,1)}^{(1,1,1)}\bar{\Pi}_{(2,1,0)}^{(1,1,1)}\bar{\Pi}_{(2,0,1)}^{(1,1,1)}\bar{\Pi}_{(1,2,0)}^{(1,1,1)}\bar{\Pi}_{(1,0,2)}^{(1,1,1)}\bar{\Pi}_{(0,2,1)}^{(1,1,1)}\bar{\Pi}_{(0,1,2)}^{(1,1,1)}\right) \\
&+\left(\frac{1}{2}\psi\right)^2 \bar{\psi}\log_2\left(\bar{\Pi}_{(1,1,0)}^{(1,1,0)}\bar{\Pi}_{(0,1,1)}^{(1,1,0)}\bar{\Pi}_{(1,0,1)}^{(1,1,0)}\bar{\Pi}_{(0,0,2)}^{(1,1,0)}\bar{\Pi}_{(1,1,0)}^{(1,0,1)}\bar{\Pi}_{(0,1,1)}^{(1,0,1)}\times\right. \\
&\qquad\left.\bar{\Pi}_{(1,0,1)}^{(1,0,1)}\bar{\Pi}_{(0,2,0)}^{(1,0,1)}\bar{\Pi}_{(1,1,0)}^{(0,1,1)}\bar{\Pi}_{(1,0,1)}^{(0,1,1)}\bar{\Pi}_{(0,1,1)}^{(0,1,1)}\bar{\Pi}_{(2,0,0)}^{(0,1,1)}\right) \\
&+\left(\frac{1}{2}\psi\right)\bar{\psi}^2\log_2\left(\bar{\Pi}_{(0,1,0)}^{(1,0,0)}\bar{\Pi}_{(0,0,1)}^{(1,0,0)}\bar{\Pi}_{(1,0,0)}^{(0,1,0)}\bar{\Pi}_{(0,0,1)}^{(0,1,0)}\bar{\Pi}_{(1,0,0)}^{(0,0,1)}\bar{\Pi}_{(0,1,0)}^{(0,0,1)}\right) \\
&+\bar{\psi}^3\log_2\left(\bar{\Pi}_{(0,0,0)}^{(0,0,0)}\right) \\
=&a\psi^3+b\psi^2+c\psi+d\equiv\mathcal{R}^{\mathrm{U}}(\psi), \qquad (3.15)
\end{aligned}
$$

where

$$
\begin{aligned}
a\equiv&\log_2\left[\left(\bar{\Pi}_{(1,1,1)}^{(1,1,1)}\bar{\Pi}_{(1,1,1)}^{(1,1,1)}\bar{\Pi}_{(2,1,0)}^{(1,1,1)}\bar{\Pi}_{(2,0,1)}^{(1,1,1)}\bar{\Pi}_{(1,2,0)}^{(1,1,1)}\bar{\Pi}_{(1,0,2)}^{(1,1,1)}\bar{\Pi}_{(0,2,1)}^{(1,1,1)}\bar{\Pi}_{(0,1,2)}^{(1,1,1)}\right)^{\frac{1}{8}}\times\right. \\
&\qquad\left.\left(\bar{\Pi}_{(0,1,0)}^{(1,0,0)}\bar{\Pi}_{(0,0,1)}^{(1,0,0)}\bar{\Pi}_{(1,0,0)}^{(0,1,0)}\bar{\Pi}_{(0,0,1)}^{(0,1,0)}\bar{\Pi}_{(1,0,0)}^{(0,0,1)}\bar{\Pi}_{(0,1,0)}^{(0,0,1)}\right)^{\frac{1}{2}}\right] \\
&-\log_2\left[\left(\bar{\Pi}_{(1,1,0)}^{(1,1,0)}\bar{\Pi}_{(0,1,1)}^{(1,1,0)}\bar{\Pi}_{(1,0,1)}^{(1,1,0)}\bar{\Pi}_{(0,0,2)}^{(1,1,0)}\bar{\Pi}_{(1,1,0)}^{(1,0,1)}\bar{\Pi}_{(0,1,1)}^{(1,0,1)}\bar{\Pi}_{(1,0,1)}^{(1,0,1)}\right)^{\frac{1}{4}}\times\right. \\
&\qquad\left.\left(\bar{\Pi}_{(0,2,0)}^{(1,0,1)}\bar{\Pi}_{(1,1,0)}^{(0,1,1)}\bar{\Pi}_{(1,0,1)}^{(0,1,1)}\bar{\Pi}_{(0,1,1)}^{(0,1,1)}\bar{\Pi}_{(2,0,0)}^{(0,1,1)}\right)^{\frac{1}{4}}\left(\bar{\Pi}_{(0,0,0)}^{(0,0,0)}\right)\right], \\
b\equiv&\log_2\left[\left(\bar{\Pi}_{(1,1,0)}^{(1,1,0)}\bar{\Pi}_{(0,1,1)}^{(1,1,0)}\bar{\Pi}_{(1,0,1)}^{(1,1,0)}\bar{\Pi}_{(0,0,2)}^{(1,1,0)}\bar{\Pi}_{(1,1,0)}^{(1,0,1)}\bar{\Pi}_{(0,1,1)}^{(1,0,1)}\bar{\Pi}_{(1,0,1)}^{(1,0,1)}\right)^{\frac{1}{4}}\times\right. \\
&\qquad\left.\left(\bar{\Pi}_{(0,2,0)}^{(1,0,1)}\bar{\Pi}_{(1,1,0)}^{(0,1,1)}\bar{\Pi}_{(1,0,1)}^{(0,1,1)}\bar{\Pi}_{(0,1,1)}^{(0,1,1)}\bar{\Pi}_{(2,0,0)}^{(0,1,1)}\right)^{\frac{1}{4}}\left(\bar{\Pi}_{(0,0,0)}^{(0,0,0)}\right)^3\right] \\
&-\log_2\left(\bar{\Pi}_{(0,1,0)}^{(1,0,0)}\bar{\Pi}_{(0,0,1)}^{(1,0,0)}\bar{\Pi}_{(1,0,0)}^{(0,1,0)}\bar{\Pi}_{(0,0,1)}^{(0,1,0)}\bar{\Pi}_{(1,0,0)}^{(0,0,1)}\bar{\Pi}_{(0,1,0)}^{(0,0,1)}\right), \\
c\equiv&\log_2\left(\bar{\Pi}_{(0,1,0)}^{(1,0,0)}\bar{\Pi}_{(0,0,1)}^{(1,0,0)}\bar{\Pi}_{(1,0,0)}^{(0,1,0)}\bar{\Pi}_{(0,0,1)}^{(0,1,0)}\bar{\Pi}_{(1,0,0)}^{(0,0,1)}\bar{\Pi}_{(0,1,0)}^{(0,0,1)}\right)^{\frac{1}{2}}-\log_2\left(\bar{\Pi}_{(0,0,0)}^{(0,0,0)}\right)^3, \\
d\equiv&\log_2\left(\bar{\Pi}_{(0,0,0)}^{(0,0,0)}\right).
\end{aligned}
$$

We determine the optimal value $\psi^\star$ that maximizes $\mathcal{R}^{\mathrm{U}}(\psi)$ in (3.15). Given that $\mathcal{R}^{\mathrm{U}}(\psi)$ is a cubic function of ψ, we consider the cases depending on a sign of a and location of poles ψ^{D1}, ψ^{D2} to determine $\psi^\star$. Considering the cases, $\psi^\star$ is determined as

(i) $a < 0$

$$\psi^\star = \begin{cases} 0 & \text{if} \quad \psi^{D1}, \psi^{D2} > 1 \\ \max\limits_{\psi} \left(\mathcal{R}^{\mathrm{U}}(0), \mathcal{R}^{\mathrm{U}}(1)\right) & \text{if} \quad 0 \leq \psi^{D1} \leq 1 \leq \psi^{D2} \\ 0 & \text{if} \quad \psi^{D1} \leq 0 \leq 1 \leq \psi^{D2} \\ \max\limits_{\psi} \left(\mathcal{R}^{\mathrm{U}}(0), \mathcal{R}^{\mathrm{U}}(\psi^{D2})\right) & \text{if} \quad 0 \leq \psi^{D1}, \psi^{D2} \leq 1 \\ \psi^{D2} & \text{if} \quad \psi^{D1} \leq 0 \leq \psi^{D2} \leq 1 \\ 0 & \text{if} \quad \psi^{D1}, \psi^{D2} < 0 \end{cases}$$

(ii) $a > 0$

$$\psi^\star = \begin{cases} 1 & \text{if} \quad \psi^{D1}, \psi^{D2} > 1 \\ \psi^{D1} & \text{if} \quad 0 \leq \psi^{D1} \leq 1 \leq \psi^{D2} \\ 1 & \text{if} \quad \psi^{D1} \leq 0 \leq 1 \leq \psi^{D2} \\ \max\limits_{\psi} \left(\mathcal{R}^{\mathrm{U}}(0), \mathcal{R}^{\mathrm{U}}(\psi^{D1})\right) & \text{if} \quad 0 \leq \psi^{D1}, \psi^{D2} \leq 1 \\ \max\limits_{\psi} \left(\mathcal{R}^{\mathrm{U}}(0), \mathcal{R}^{\mathrm{U}}(1)\right) & \text{if} \quad \psi^{D1} \leq 0 \leq \psi^{D2} \leq 1 \\ 1 & \text{if} \quad \psi^{D1}, \psi^{D2} < 0, \end{cases}$$

$$\begin{aligned} \text{where} \quad & \psi^{D1} = (-b - \sqrt{b^2 - 3ac})/3a, \ \psi^{D2} = (-b + \sqrt{b^2 - 3ac})/3a \\ & \text{s.t.} \ \left[\frac{\partial \mathcal{R}^{\mathrm{U}}(\psi)}{\partial \psi}\right]_{\psi = \psi^{D1}, \psi^{D2}} = 0. \end{aligned} \tag{3.16}$$

Then, we can determine the optimal value of global selfishness $\lambda^\star$ by using $\psi^\star$. Since $||\mathbf{h}_{ji}||^2$ has a Gamma(N_t,2) distribution and there is one-to-one correspondence between ψ and λ, $\lambda^\star$ can be uniquely determined with $\psi^\star$ and derived as

$$\lambda^\star = F^{-1}(1 - \psi^\star; N_t, 2). \tag{3.17}$$

Table 3.2: BS_1 actions and Corresponding Probabilities in Three-Sectored Cellular Network

Case #	BS_1 action	Probability
Case 1	Egoistic	$\bar{\psi}$
Case 2	Altruistic for MS_2	$(1/2)\psi$
Case 3	Altruistic for MS_3	$(1/2)\psi$

3.3.3 Practical Cellular Network Scenario with N_t antennas

We extend our scheme to a general multicell networks. In the previous subsections, we derived our beamforming scheme considering ideal two-cell and practical three-sectored cellular network assuming two transmit antennas. However, it can be easily expended for general N_t antennas system. In the previous subsection, the proposed one-shot beamforming scheme makes each BS nullifies the one of the interference links since we consider that each BS has two transmit antennas. When each BS has $N_t \geq 3$ transmit antennas, the probability of BS actions are modified. Taking BS_1 as an example, we describe actions of BS_1 and corresponding probabilities in Table 3.3. Therefore, there are a total of $4^3 = 64$ different cases for three-sectored networks with N_t antennas. Then, we can derive the expectation of sum rate by using probabilities and corresponding sum rate analysis in the same way of (3.10) and (3.14).

$$
\begin{aligned}
&\mathbb{E}[\mathcal{R}(\psi)] \\
\leq&\psi^6 \log_2\left(\bar{\Pi}^{(2,2,2)}_{(2,2,2)}\right) + \psi^5\bar{\psi}\log_2\left(\bar{\Pi}^{(2,2,1)}_{(2,1,2)}\bar{\Pi}^{(2,2,1)}_{(1,2,2)}\bar{\Pi}^{(2,1,2)}_{(1,2,2)}\bar{\Pi}^{(2,1,2)}_{(2,2,1)}\bar{\Pi}^{(1,2,2)}_{(2,1,2)}\bar{\Pi}^{(1,2,2)}_{(2,2,1)}\right) \\
&+ \psi^4\bar{\psi}^2\log_2\Big(\bar{\Pi}^{(2,1,1)}_{(2,1,1)}\bar{\Pi}^{(2,1,1)}_{(0,2,2)}\bar{\Pi}^{(2,1,1)}_{(1,2,1)}\bar{\Pi}^{(2,1,1)}_{(1,1,2)}\bar{\Pi}^{(1,2,1)}_{(1,2,1)}\bar{\Pi}^{(1,2,1)}_{(2,0,2)}\bar{\Pi}^{(1,2,1)}_{(2,1,1)}\times \\
&\qquad\qquad \bar{\Pi}^{(1,2,1)}_{(1,1,2)}\bar{\Pi}^{(1,1,2)}_{(1,1,2)}\bar{\Pi}^{(1,1,2)}_{(2,2,0)}\bar{\Pi}^{(1,1,2)}_{(2,1,1)}\bar{\Pi}^{(1,1,2)}_{(1,2,1)}\bar{\Pi}^{(2,2,0)}_{(1,1,2)}\bar{\Pi}^{(2,0,2)}_{(1,2,1)}\bar{\Pi}^{(0,2,2)}_{(2,1,1)}\Big) \\
&+ \psi^3\bar{\psi}^3\log_2\Big(\bar{\Pi}^{(1,1,1)}_{(2,1,0)}\bar{\Pi}^{(1,1,1)}_{(2,0,1)}\bar{\Pi}^{(1,1,1)}_{(1,2,0)}\bar{\Pi}^{(1,1,1)}_{(1,0,2)}\bar{\Pi}^{(1,1,1)}_{(0,1,2)}\bar{\Pi}^{(1,1,1)}_{(0,1,2)}\bar{\Pi}^{(1,1,1)}_{(1,1,1)}\bar{\Pi}^{(1,1,1)}_{(1,1,1)}\times \\
&\qquad\qquad \bar{\Pi}^{(2,1,0)}_{(1,1,1)}\bar{\Pi}^{(2,1,0)}_{(0,1,2)}\bar{\Pi}^{(2,0,1)}_{(1,1,1)}\bar{\Pi}^{(2,0,1)}_{(0,2,1)}\bar{\Pi}^{(1,2,0)}_{(1,1,1)}\bar{\Pi}^{(1,2,0)}_{(1,0,2)}\bar{\Pi}^{(1,0,2)}_{(1,1,1)}\bar{\Pi}^{(1,0,2)}_{(1,2,0)}\times \\
&\qquad\qquad \bar{\Pi}^{(0,1,2)}_{(1,1,1)}\bar{\Pi}^{(0,1,2)}_{(2,1,0)}\bar{\Pi}^{(0,2,1)}_{(1,1,1)}\bar{\Pi}^{(0,2,1)}_{(2,0,1)}\Big) \\
&+ \psi^2\bar{\psi}^4\log_2\Big(\bar{\Pi}^{(1,1,0)}_{(1,1,0)}\bar{\Pi}^{(1,1,0)}_{(0,1,1)}\bar{\Pi}^{(1,1,0)}_{(0,0,2)}\bar{\Pi}^{(1,1,0)}_{(1,0,1)}\bar{\Pi}^{(0,1,1)}_{(0,1,1)}\bar{\Pi}^{(0,1,1)}_{(1,0,1)}\bar{\Pi}^{(0,1,1)}_{(2,0,0)}\times \\
&\qquad\qquad \bar{\Pi}^{(0,1,1)}_{(1,1,0)}\bar{\Pi}^{(1,0,1)}_{(1,0,1)}\bar{\Pi}^{(1,0,1)}_{(0,1,1)}\bar{\Pi}^{(1,0,1)}_{(0,2,0)}\bar{\Pi}^{(1,0,1)}_{(1,1,0)}\bar{\Pi}^{(2,0,0)}_{(0,1,1)}\bar{\Pi}^{(0,2,0)}_{(1,0,1)}\bar{\Pi}^{(0,0,2)}_{(1,1,0)}\Big) \\
&+ \psi\bar{\psi}^5\log_2\left(\bar{\Pi}^{(1,0,0)}_{(0,1,0)}\bar{\Pi}^{(1,0,0)}_{(0,0,1)}\bar{\Pi}^{(0,1,0)}_{(1,0,0)}\bar{\Pi}^{(0,1,0)}_{(0,0,1)}\bar{\Pi}^{(0,0,1)}_{(1,0,0)}\bar{\Pi}^{(0,0,1)}_{(0,1,0)}\right) + \psi^6\log_2\left(\bar{\Pi}^{(0,0,0)}_{(0,0,0)}\right) \\
\equiv&\mathcal{R}^{\mathrm{U}}(\psi). \qquad (3.18)
\end{aligned}
$$

Here, $\mathcal{R}^{\mathrm{U}}(\psi)$ in (3.18) is an equation of ψ and we can determine the $\psi^{\star}$ that maximizes $\mathcal{R}^{\mathrm{U}}(\psi)$. Then, we can determine $\lambda^{\star}$ by using $\psi^{\star}$. Since $||\mathbf{h}_{ji}||^2$ has a Gamma(N_t,2) distribution and there is one-to-one correspondence between ψ and λ, $\lambda^{\star}$ can be uniquely determined with $\psi^{\star}$ and derived as

$$\lambda^{\star} = F^{-1}(1 - \psi^{\star}; N_t, 2). \tag{3.19}$$

In this scenario, it is shown that our scheme can be expanded to general N_t antennas scenario though it is not possible to find the closed-form solution for (3.19) unlike above two scenarios.

Table 3.3: BS_1 actions and Corresponding Probabilities for N_t transmit antennas

Case #	BS_1 action	Probability
Case 1	Egoistic	$\bar{\psi}^2$
Case 2	Altruistic for MS_2	$\bar{\psi}\psi$
Case 3	Altruistic for MS_3	$\bar{\psi}\psi$
Case 4	Altruistic for MS_2 and MS_3	ψ^2

3.4 Numerical Results

We evaluate the performance of the proposed one-shot cooperative beamforming. The average channel gain between the BS in the i^{th} cell and the MS in the j^{th} cell is defined as $E\left[|\mathbf{h}_{ij}|^2\right] = \rho_0 \left(d_{i,j}/d_r\right)^{-\alpha}$, where $d_{i,j}$ denotes the distance between the BS in the i^{th} cell and the MS in the j^{th} cell, and ρ_0 denotes the SNR. The reference distance d_r can be regarded as the cell radius. The values of d_r, the pathloss exponent α are set to 500m and 3.7, respectively.

Figure 3.2 shows how the optimal global selfishness $\lambda^\star$ varies with the distance of a MS from a BS, when SNR is 10dB and 30dB. When MS_1 and MS_2 are located from $0.5R$ to R by $0.1R$ interval, where R denotes the cell radius. The results of analysis are computed from the average sum rate approximation while the results of real channel are exhaustively searched from average sum rate observations with real channel realizations. Despite a slight overestimation of $\lambda^\star$, our analysis provides a computationally efficient way to determine $\lambda^\star$. When a MS is located near a BS, the optimal value of λ becomes high, which implies that each cell may act selfishly. As a MS moves toward the cell edge, the optimal value of λ gradually decreases and each cell should act altruistically. Moreover, as we expect, when SNR is 30dB, the optimal value of λ is less than 10dB since influence of interference is increased.

In Figure 3.3 and Figure 3.4, we assume an idealized two-cell network scenario and compare the average sum rate performance and cumulative distribution of user rate of the proposed one-shot beamforming scheme with those of conventional cooperative beamforming schemes, i.e., egoistic beamforming (MRT) and altruistic beamforming (ZF), V-SINR based eigen beamforming in [29] and iterative Pareto optimal beamforming in [18]. BSs equip two transmit antennas and MSs equip single antenna. MSs are randomly located in between $0.5R$ and R.

In Figure 3.3, the proposed one-shot beamforming outperforms both altruistic and egoistic beamformings in all SNR values. This is because the proposed one-shot beamforming attempts to balance the egoism and altruism with the help of the decision met-

ric, i.e., global selfishness. As compared to V-SINR based eigen beamforming, our proposed beamforming outperforms V-SINR based eigen beamforming in high SNR region. The performance of the proposed one-shot beamforming achieves about 95% of average sum rate performance of the iterative Pareto optimal beamforming. Moreover, the proposed one-shot beamforming offers substantial reduction in computational burden. In Figure 3.4, the proposed beamforming scheme outperforms other non-iterative schemes in the performance of cell edge users. As compared to V-SINR based eigen beamforming, the sum rate performance of the proposed scheme similar to that of V-SINR based eigen beamforming scheme in average sum rate performance. However, in the performance of cell edge users, the proposed beamforming scheme outperforms V-SINR based eigen beamforming scheme. This is because V-SINR based eigen beamforming scheme assumes high SINR unlike the proposed beamforming scheme.

In Figure 3.5 - 3.8, we compare the average sum rate performance and cumulative distribution of user rate in a practical three-sectored network scenario. BSs equip two transmit antennas in Figure 3.5 and Figure 3.6, while BSs equip four transmit antennas in Figure 3.7 and Figure 3.8. MSs equip single antenna and are randomly located in between $0.5R$ and R. The performance of the proposed beamforming is compared to those of egoistic beamforming, altruistic beamforming, V-SINR based eigen beamforming in [29] and iterative Pareto optimal beamforming in [25]. In Figure 3.5 and Figure 3.7, as already shown in an ideal two-cell network scenario, the proposed one-shot beamforming outperforms both altruistic and egoistic beamformings in all SNR values. As compared to iterative Pareto optimal beamforming in [25], the performances of the proposed one-shot beamforming achieves 96% and 92% of average sum rate performance of the iterative Pareto optimal beamforming in Figure 3.5 and Figure 3.7, respectively. Moreover, the proposed one-shot beamforming can reduce substantial computational burden since the iterative Pareto optimal beamforming scheme in [25] requires over 70 iterations. Compared to the V-SINR based eigen beamforming in high SNR region where ICI limits the performance, the proposed one-

shot beamforming outperforms the sum rate performances in Figure 3.5 and Figure 3.7 by 8% and 10%, respectively. The performance improvement of the proposed one-shot beamforming over V-SINR eigen beamforming becomes larger for cell edge users as shown in Figure 3.6 and Figure 3.8. The V-SINR based eigen beamforming requires some assumptions, e.g., high SINR, which is not required in the proposed beamforming. Moreover, V-SINR based eigen beamforming scheme aims to maximize sum of V-SINR metric instead of sum rate metric. Whereas, the proposed beamforming focuses on the average sum rate metric to be valid for general $M > 2$ network scenarios. The gap between sum of V-SINR metric and sum rate metric becomes larger in general $M > 2$ cases. Thus, the proposed beamforming scheme can be easily extended to any $M > 2$ network scenarios and outperforms the V-SINR based eigen beamforming in cell edges and general $M > 2$ network scenarios. This makes our approach more appropriate for practical cellular applications.

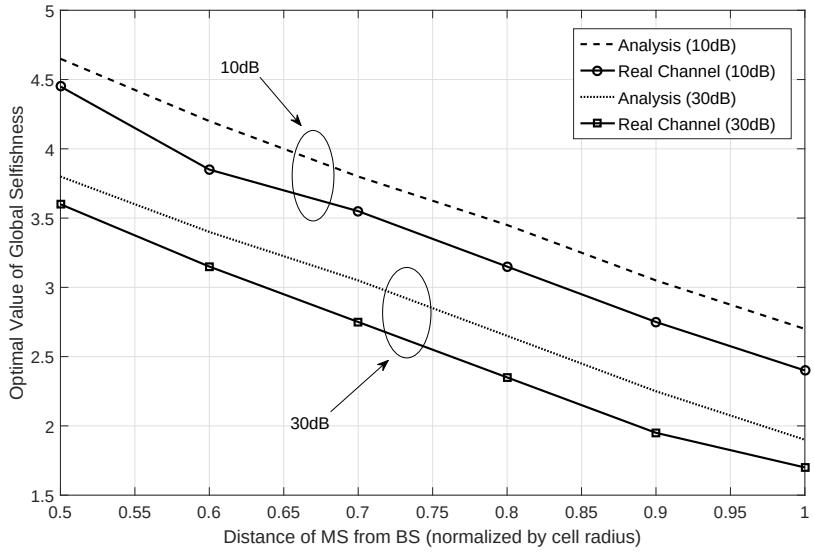

Figure 3.2: Optimal global selfishness λ versus distance of MS from BS

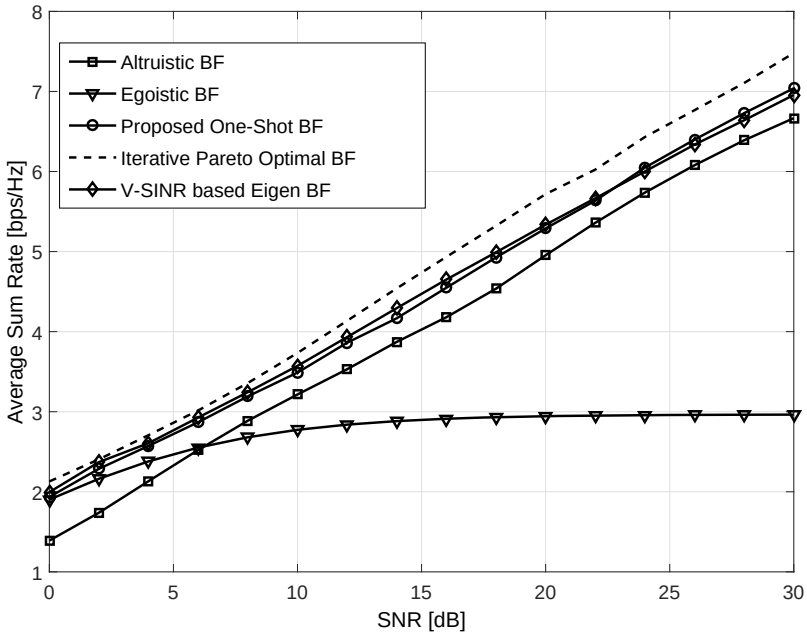

Figure 3.3: Average sum rate versus SNR in an ideal two-cell network scenario.

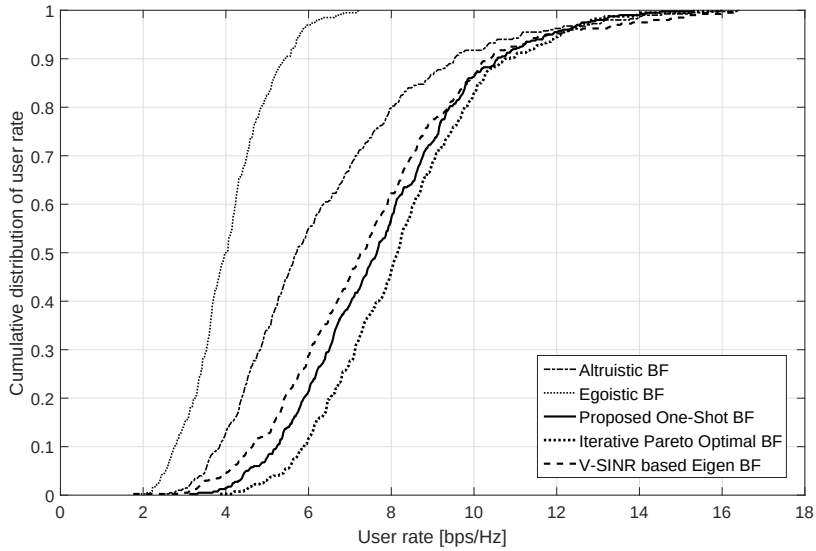

Figure 3.4: Cumulative distribution of user rate versus user rate in an ideal two-cell network scenario, when SNR=30dB.

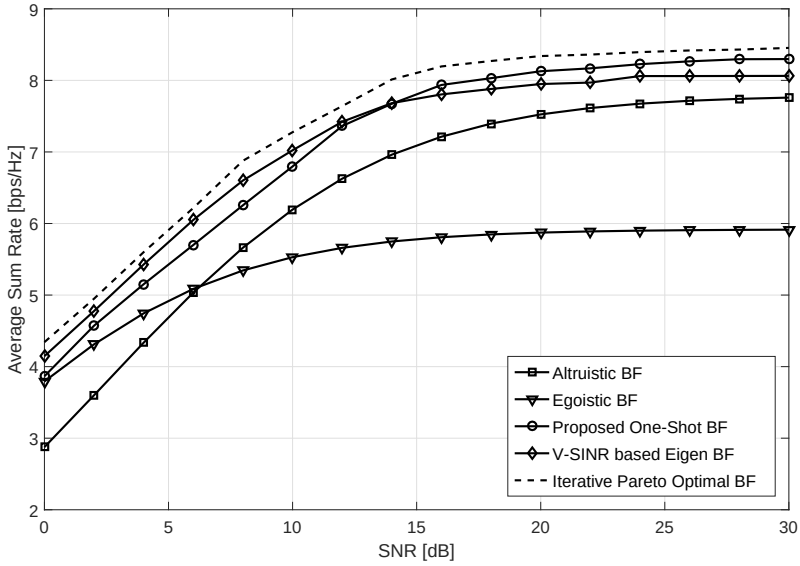

Figure 3.5: Average sum rate versus SNR in a practical three-sectored cellular network scenario.

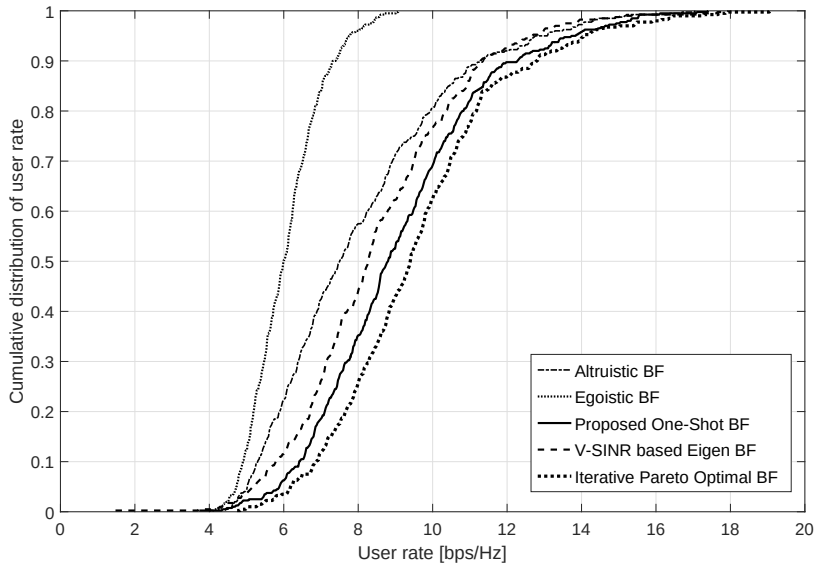

Figure 3.6: Cumulative distribution of user rate versus user rate in a practical three-sectored cellular network scenario, when SNR=30dB.

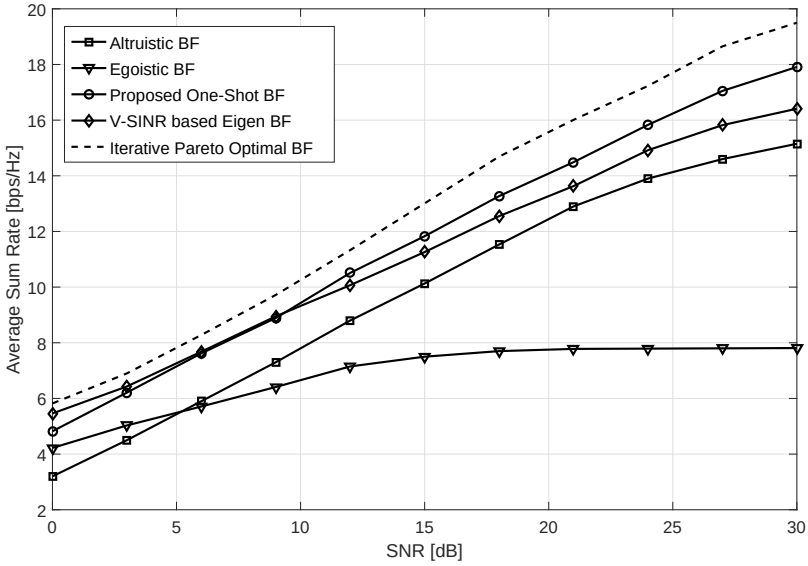

Figure 3.7: Average sum rate versus SNR in a practical three-sectored cellular network scenario with N_t=4.

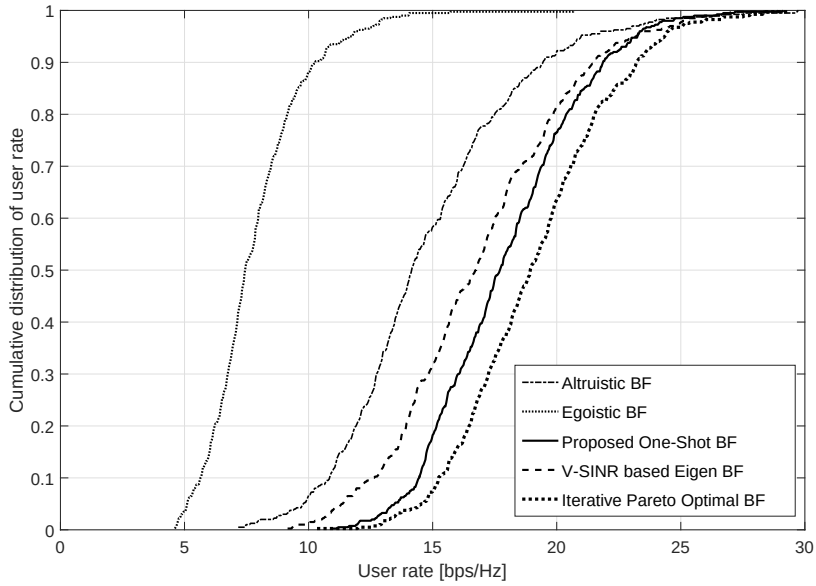

Figure 3.8: Cumulative distribution of user rate versus user rate in a practical three-sectored cellular network scenario with N_t=4, when SNR=30dB.

Chapter 4

Distributed Cell Clustering Algorithm Based on Message Passing

4.1 System Model

We consider a downlink cellular system comprised of M cells. We assume that single mobile station (MS) in each cell is already selected to be served by scheduler. Each BS is equipped with N_t antennas and the MS has a single antenna. The received signal vector $\mathbf{y}_i$ at the MS in the i^{th} cell can be expressed as

$$\mathbf{y}_i = \sqrt{\rho_i}\mathbf{h}_{ii}\mathbf{w}_i\mathbf{x}_i + \sum_{j=1, j\neq i}^{M} \sqrt{\rho_{ji}}\mathbf{h}_{ji}\mathbf{w}_j\mathbf{x}_j + \mathbf{n}_i, \tag{4.1}$$

where $\mathbf{h}_{ji}$ denotes $1 \times N_t$ channel vector between BS in the j^{th} cell and the MS in the i^{th} cell, $\mathbf{w}_i$ denotes $N_t \times 1$ corresponding beamforming vector at the BS in the i^{th} cell, and it is normalized, i.e., $||\mathbf{w}_i||^2 = 1$. $\mathbf{x}_i$ is the signal transmitted from the i^{th} BS to the i^{th} MS. We assume that the elements of $\mathbf{h}_{ji}$ follow independent and identically distributed complex Gaussian distribution with zero mean and unit variance. In addition, $\mathbf{n}_i$ denotes the additive white Gaussian noise (AWGN) at the i^{th} MS with unit variance, ρ_i denotes the average signal-to-noise ratio (SNR) of the MS in the i^{th} cell, and ρ_{ji} is the average interference-to-noise ratio (INR) for the interference that the BS

in the j^{th} cell causes to the MS in the i^{th} cell. The received SINR γ_i of the MS in the i^{th} cell can be computed from (4.1) as

$$\gamma_i = \frac{\rho_i |\mathbf{h}_{ii}\mathbf{w}_i|^2}{1 + \sum\limits_{j=1, j\neq i}^{M} \rho_{ji} |\mathbf{h}_{ji}\mathbf{w}_j|^2}. \tag{4.2}$$

From (4.2), the network-wide sum rate of all cells $\mathcal{R}$ is given as

$$\mathcal{R} = \sum_{i=1}^{M} \log_2 (1 + \gamma_i). \tag{4.3}$$

4.2 Message Passing Algorithm

In this section, we develop message passing algorithm for distributed cell clustering. For message derivations, we define a parameter γ_{ij} is called CoMP gain and it can be expressed as

$$\gamma_{ij} = \sum_{k\in\{i,j\}} R_k^C - \sum_{k\in\{i,j\}} R_k^{non}, \gamma_{ii} = 0. \tag{4.4}$$

γ_{ij} denotes the CoMP gain. R_k^C represents the rate of k^{th} MS when k^{th} BS operates in cooperative manner and R_k^{non} represents the rate of k^{th} MS when k^{th} BS operates with no cooperation. We define integer variable $x_i \in \{1, 2, ..., M\}$ is introduced to specify the BS index for which BS cooperates with. Note that $x_i = i$ corresponds to the case where the i^{th} BS operates with no cooperation. In addition, indicator function $\chi_i(x_j)$ is defined to yield one, if the j^{th} BS cooperates with i^{th} BS, and zero, otherwise. We assume that each BS cooperates with only one BS since the sum rate metric is all coupled. Therefore, we simplified the sum rate problem and repeat the algorithm for cell clustering. Since each BS cooperates with at most one BS, a constraint is imposed such that the number of BS should not exceed the number of cooperation. Therefore, a formulation for clustering of the best pairing and its optimal resource allocation is

given by

$$\textbf{maximize} \sum_{\mathbf{i}} \sum_{\mathbf{j}} \gamma_{\mathbf{ij}} \chi_{\mathbf{i}}(\mathbf{x_j})$$

$$\textbf{subject to} \sum_{\mathbf{j} \in \mathbf{B(i)}} \chi(\mathbf{x_j}) \leq \chi(\mathbf{x_i}),\ \forall \mathbf{i},$$

$$x_i \in \{1, 2, ..., M\} \tag{4.5}$$

where $B(i)$ denotes the set of adjacent BSs of the i^{th} BS. For $x_i = i$ the constraint forces someone else to cooperate with the i^{th} BS, if the equality holds, and leaves the i^{th} BS alone, if inequality holds. For $x_i \neq i$, the i^{th} BS becomes a cooperations and nobody cooperates with the i^{th} BS. Therefore, each BS should either act in cooperation manner or leave alone with no cooperation.

Solving the combination problem (4.5) places computationally intractable load on centralized control policy, which highlights the need for a simple distributed approach. Therefore, we develop the message passing algorithm for distributed approach. For message passing algorithm, (4.5) is reformulated as an unconstrained problem

$$\max_{\{x_i\}} \sum_{j} S_j(x_j) + \sum_{i} F_i(\mathbf{X}_i), \tag{4.6}$$

where $\mathbf{X}_i = \{x_j : j \in B(i)\}$, and $F_i(\mathbf{X}_i)$ is defined to enforce the constraint in (4.5) as

$$F_i(\mathbf{X}_i) = \begin{cases} -\infty & if \sum_{j \in B(i)} \chi_i(x_j) > \chi_i(x_i) \\ 0 & otherwise \end{cases} \tag{4.7}$$

The contribution of variable x_j to objective is expressed as $S_j(x_j) = \sum_i \gamma_{ij} \chi_i(x_j)$. Message passing algorithm solves (4.6) via message exchanges over the nodes, thereby yielding a distributed solution. Since messages are exchanged along all edges in two oppsite directions, two different types of messages are defined. The messages represent preference of the best value that x_j takes.

We derive the message update rules that solve (4.5). Two types of messages are exchanged between variable node x_j and function node $\mathbf{F_i}$. Messages λ_{ij} and μ_{ij}

denotes messages from variables and from functions, respectively. Let $\tilde{\lambda_{ij}}$ and $\tilde{\mu_{ij}}$ denote the preference for the former cases, whereas the preferences for the latter cases are denoted by $\bar{\lambda_{ij}}$ and $\bar{\mu_{ij}}$. According to the max-sum rule for variables, the message transferred from x_j to $\mathbf{F_i}$ is given by the preference of the j^{th} BS cooperates with the i^{th} BS minus maximum among preferences of the i^{th} BS cooperates with other BSs, which is obtaining using

$$\begin{aligned}\lambda_{ij} \equiv \tilde{\lambda}_{ij} - \bar{\lambda}_{ij} &= \gamma_{ij} + \sum_{k \in B(j)\backslash i} \bar{\mu}_{kj} - \max_{k \in B(j)\backslash i} \left(\gamma_{kj} + \tilde{\mu}_{kj} + \sum_{l \in B(j)\backslash \{i,k\}} \bar{\mu}_{lj} \right) \\ &= \gamma_{ij} - \max_{k \in B(j)\backslash i} (\gamma_{kj} + \mu_{kj}) \end{aligned} \tag{4.8}$$

On the other hand, the message transferred from $\mathbf{F_i}$ to x_j differs according to i. If $i = j$, the message is defined as the difference between the maximal preference that at most one neighbor BS of the i^{th} BS cooperates with the i^{th} BS and $\bar{\mu}_{ii}$ indicating no BS cooperating, Therefore, the message is simply given by

$$\begin{aligned}\mu_{ii} \equiv &\tilde{\mu}_{ii} - \bar{\mu}_{ii} = \max_{k \in B(i)} \left(\max \left(\tilde{\lambda}_{ik}, \bar{\lambda}_{ik} \right) + \sum_{l \in B(i)\backslash k} \bar{\lambda}_{il} \right) \\ &- \sum_{k \in B(i)} \bar{\lambda}_{ik} = \max_{k \in B(i)} \max(0, \lambda_{ik}) \end{aligned} \tag{4.9}$$

If $i \neq j$, $\tilde{\mu}_{ij}$ is associated with the case where the j^{th} BS cooperates with the i^{th} BS. In addition, $\bar{\mu}_{ij}$ corresponds to case where the other BS cooperate with the i^{th} BS. The corresponding message is derived as

$$\begin{aligned}\mu_{ij} \equiv \tilde{\mu}_{ij} - \bar{\mu}_{ij} &= \tilde{\lambda}_{ii} + \sum_{k \in B(i)\backslash j} \bar{\lambda}_{ik} \\ &\quad - \max \left(\bar{\lambda}_{ii} + \sum_{k \in B(i)\backslash j} \bar{\lambda}_{ik}, \max_{k \in B(i)\backslash j} \left(\max \left(\tilde{\lambda}_{ik}, \bar{\lambda}_{ik} \right) + \sum_{l \in B(i)\backslash \{k,j\}} \bar{\lambda}_{jl} \right) \right) \\ &= \min \left(\lambda_{ii}, - \max_{k \in B(i)\backslash j} \max(0, \lambda_{ik}) \right) \end{aligned} \tag{4.10}$$

The overall iterative message update rules can be expressed as

$$\mu_{ij}^{(t)} = \begin{cases} \max\limits_{k \in B(i)} \left(\lambda_{ik}^{(t)}, 0 \right) & \text{if } i = j \\ \min \left(\lambda_{ii}^{(t)}, - \max\limits_{k \in B(i) \setminus j} \max \left(\lambda_{ik}^{(t)}, 0 \right) \right) & \text{o.w} \end{cases}$$

$$\lambda_{ij}^{(t+1)} = \gamma_{ij} - \max_{k \in B(j) \setminus i} \left(\gamma_{kj} + \mu_{kj}^{(t)} \right), \tag{4.11}$$

The clustering can be determined by

$$\hat{x}_j^{(t)} = \arg\max_i \left(\mu_{ij}^{(t)} + \lambda_{ij}^{(t)} \right), \tag{4.12}$$

and the corresponding decisions are made such that (i) if $\hat{x}_j^{(t)} = i$, the j^{th} BS cooperates with the i^{th} BS; and (ii) if $\hat{x}_j^{(t)} = j$ the j^{th} BS operates alone.

4.3 Numerical Results

We evaluate the performance of the proposed cell clustering algorithm. We consider M cell model with N_t = 2 and N_r =1. The pathloss exponent is set to 3.7 in the simulations.

In Figure 4.1 - 4.4 , we compare the average sum rate performances of conventional cell clustering algorithms, i.e. optimal exhaustive search algorithm and distributed cell clustering algorithm [43]. The MSs are located in between $0.5R$ and R. We compare the performances for JP-CoMP systems in Figure 4.1 and 4.2, for CS/CB-CoMP systems in Figure 4.3 and 4.4. We illustrate the sum rate performances varies the number of cells in Figure 4.1 and 4.3. Figure 4.2 and 4.4 show the performance varies edge SNR of users. The proposed clustering algorithm outperforms the conventional distributed algorithm. This is because the proposed clustering algorithm attempts to derive messages for self clustering. Compared to exhaustive search algorithm, considering the substantial reduction in computational burden, the proposed clustering algorithms is appropriate for practical implementations in cellular networks.

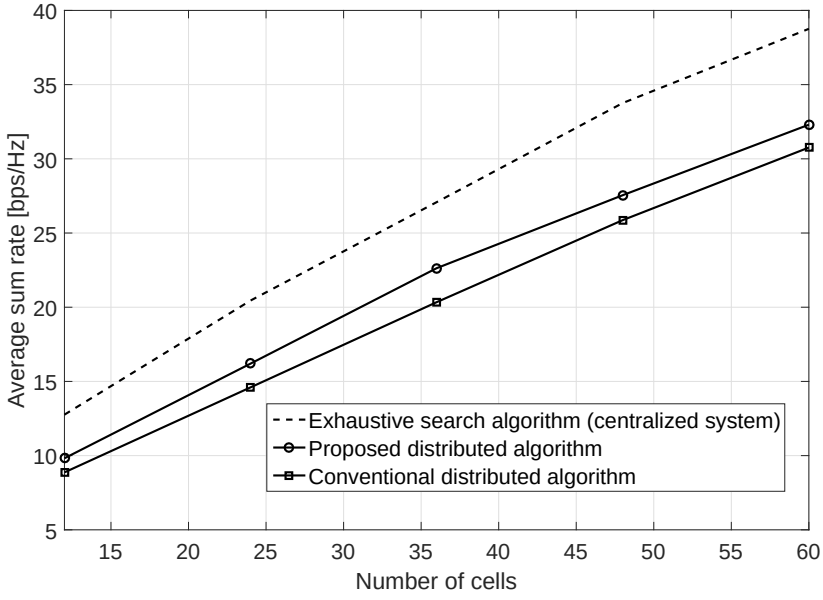

Figure 4.1: Average sum rate versus Number of cells in CoMP-JP systems.

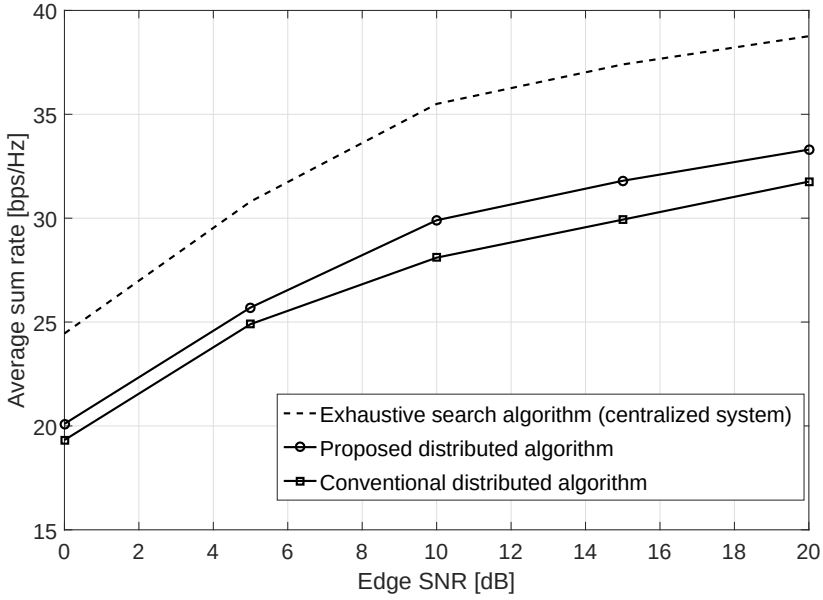

Figure 4.2: Average sum rate versus edge SNR in CoMP-JP systems.

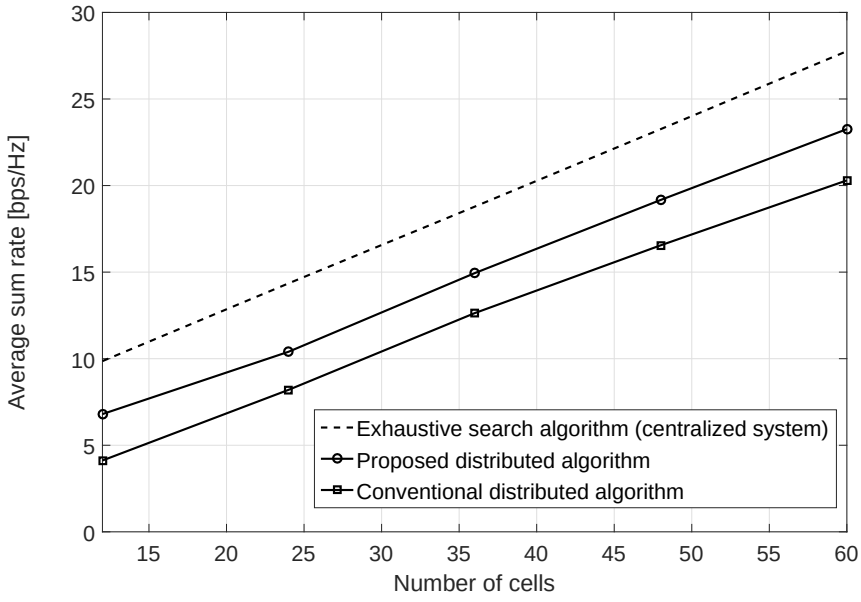

Figure 4.3: Average sum rate versus Number of cells in CoMP-CS/CB systems.

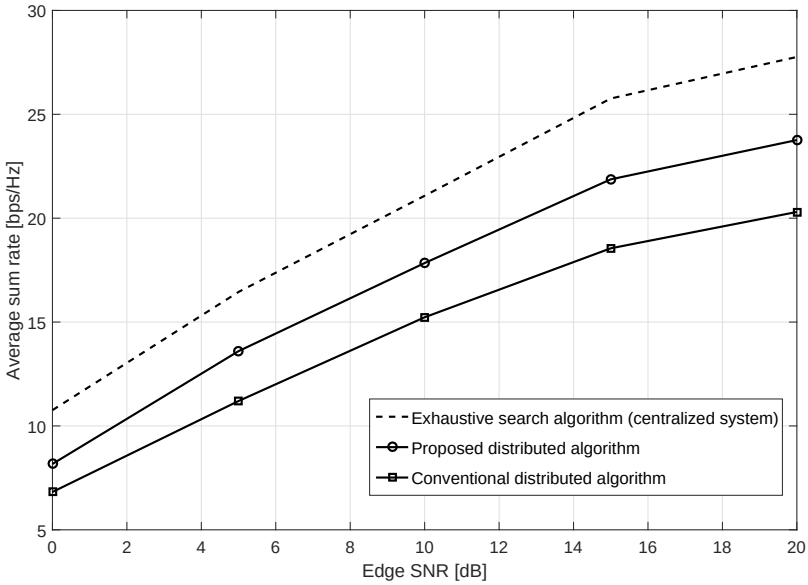

Figure 4.4: Average sum rate versus edge SNR in CoMP-CS/CB systems.

Chapter 5

Conclusion

In the first part of this dissertation, we have proposed a successive user selection scheme for the downlink of MIMO cellular systems in a multicell environment. The proposed scheme works jointly with SGINR beamforming and attempts to maximize the sum rate over all of the users in a cluster of cells. As compared to the optimal exhaustive search, the proposed scheme is much less complex due to the derivation of a simple incremental metric for the sum rate. Numerical results confirm that the proposed user selection scheme achieves a sum rate close to that of the exhaustive search. In a particular case, the proposed scheme has been shown to achieve 94% of the sum rate of the exhaustive search, while reduction in computational complexity amounts to about 26,600 fold. In the second part of this dissertation, we have proposed a one-shot cooperative beamforming for downlink multicell systems. Unlike conventional non-iterative approaches, we focus the average sum rate metric and determine optimal global selfishness that maximizes sum rate. By using predetermined global selfishness, each BS can autonomously determine whether it behave selfishly or altruistically. The main contributions of this paper are (i) the closed-form derivations of the global selfishness that maximizes average sum rate, (ii) the practical solution for typical three-sectored cellular networks, and (iii) considerable performance improvement especially for cell edge users. Future research direction will include multi-users, multi-

antennas at users, heterogeneous networks, etc. In the third part of this dissertation, we have proposed the distributed cell clustering algorithm for multicell CoMP systems. As compared to the optimal exhaustive search algorithm, the proposed algorithm reduces substantial computational complexity due to the distributed process. Numerical results confirm that proposed clustering algorithm has been shown to achieve 84% of the average sum rate of the exhaustive search algorithm, while reduction in computational complexity. Moreover, the sum rate performance outperforms the conventional distributed algorithm.

Appendix

Appendix A

There exists two cases for $\Gamma_i^{(e_i,a_i)}$ depending on the choice of interference links nulling. In the first case, the received interference link is nullified by neighboring BS. Therefore, $\Gamma_i^{(e_i,a_i)}$ can be expressed as

$$\Gamma_i^{(e_i,1)} = 1 + \rho_i \chi^2_{2(N_t-e_i)} \quad i = 1, 2. \tag{5.1}$$

The expectation of (5.1) is derived as follows

$$\mathbb{E}\left[\Gamma_i^{(e_i,1)}\right] = 1 + 2\rho_i(N_t - e_i). \tag{5.2}$$

In the second case, the received interference link is not nullified by other BS and then, $\Gamma_i^{(e_i,a_i)}$ can be expressed as

$$\Gamma_i^{(e_i,0)} = 1 + \frac{\rho_i \chi^2_{2(N_t-e_i)}}{1 + \rho_{ji}\chi^2_2} \quad i, j \in \{1, 2\},\ i \neq j. \tag{5.3}$$

For calculating the expectation of $\Gamma_i^{(e_i,0)}$ in (5.3), we define random variable $X \equiv \frac{\alpha Z}{1+\beta Y}$, where the random variable $Z \sim \chi^2_{2K}$ and $Y \sim \chi^2_2$. α and β are real-value coefficients. Since Y and Z are independent, the cdf of X can be derived as

$$F_X(x) = 1 - \sum_{n=0}^{K-1} \sum_{l=0}^{n} \frac{\alpha^{l+1-n}}{\beta(n-l)!} \cdot \frac{x^n e^{-x/\alpha}}{(x + \alpha/\beta)^{l+1}}. \tag{5.4}$$

Then, the expectation of X is derived as follows

$$\begin{aligned}\mathbb{E}[X] &= \int_0^\infty x dF_X = \int_0^\infty 1 - F_X(x) dx \\ &= \sum_{n=0}^{K-1} \sum_{l=0}^{n} \frac{\alpha^{l+1-n}}{\beta(n-l)!} \int_0^\infty \frac{x^n e^{-x/\alpha}}{(x+\alpha/\beta)^{l+1}} dx. \end{aligned} \tag{5.5}$$

The expression of integral in (5.5) is derived as

$$\int_0^\infty \frac{x^n e^{-x/\alpha}}{(x+\alpha/\beta)^{l+1}} dx = e^{-\beta} \sum_{k=0}^{n} \binom{n}{k} (-\alpha/\beta)^{n-k} \int_{\alpha/\beta}^\infty x^{k-l-1} e^{-x/\alpha} dx. \tag{5.6}$$

The integral in (5.6) can be given as

$$\begin{aligned} R(\alpha, \beta | p) &= \int_{\alpha/\beta}^\infty x^p e^{-x/\alpha} dx \\ &= \begin{cases} e^{-1/\beta} \sum\limits_{i=0}^{p} \frac{p!}{i!} \frac{\alpha^{2i-p-1}}{\beta^i} & \text{if } p \geq 0 \\ E_1(1/\beta) & \text{if } p = -1 \\ \frac{(-\alpha)^{p+1} E_1(1/\beta)}{(-p-1)!} + e^{-1/\beta} \left(\frac{\alpha}{\beta}\right)^{p+1} \sum\limits_{i=0}^{-p-2} \frac{(-p-i-2)!}{(-\beta)^i (-p-1)!} & \text{if } p \leq -2, \end{cases} \end{aligned} \tag{5.7}$$

where $p = k - l - 1$ and $E_1(\cdot)$ is the first order exponential-integral function.

Appendix B

In Practical three-sectored scenario, there are three cases for $\Gamma_i^{(e_i,a_i)}$ depending on the choice of interference link nulling. In the first case, all the received interference links are nullified by neighboring BSs. In the second case, one interference link is nullified and the other is not nullified. The derivations of the first and the second cases are equal to those of ideal two-cell scenario as derived in Appendix A. In the third case, all the interference links are not nullified by neighboring BSs. Therefore, $\Gamma_i^{(e_i,a_i)}$ can be expressed as

$$\Gamma_i^{(e_i,0)} = 1 + \frac{\rho_i \chi^2_{2(N_t - e_i)}}{1 + \rho_{ji} \chi_2^2 + \rho_{ki} \chi_2^2} \quad i,j,k \in \{1,2,3\},\ i \neq j \neq k. \tag{5.8}$$

For the calculations of the expectation, we define random variable $X \equiv \frac{\alpha Z}{1+\beta_1 Y_1+\beta_2 Y_2}$, where the random variable $Z \sim \chi^2_{2K}$, $Y_1 \sim \chi^2_2$ and $Y_2 \sim \chi^2_2$. α, β_1 and β_2 are real-value coefficients. Since the random variables are independent, the cdf of X can be derived as

$$F_X(x) = 1 - \sum_{n=0}^{K-1} \sum_{l=0}^{n} \frac{\alpha^{l+1-n}}{(\beta_1-\beta_2)(n-l)!} \left(\frac{x^n e^{-x/\alpha}}{(x+\alpha/\beta_1)^{l+1}} - \frac{x^n e^{-x/\alpha}}{(x+\alpha/\beta_2)^{l+1}} \right). \tag{5.9}$$

Then, the expectation of X is derived as

$$\begin{aligned}
\mathbb{E}[X] &= \int_0^\infty x dF_X = \int_0^\infty 1 - F_X(x) dx \\
&= \sum_{n=0}^{K-1} \sum_{l=0}^{n} \frac{\alpha^{l+1-n}}{(\beta_1-\beta_2)(n-l)!} \left(\int_0^\infty \frac{x^n e^{-x/\alpha}}{(x+\alpha/\beta_1)^{l+1}} dx - \int_0^\infty \frac{x^n e^{-x/\alpha}}{(x+\alpha/\beta_2)^{l+1}} dx \right) \\
&= \sum_{n=0}^{K-1} \sum_{l=0}^{n} \frac{\alpha^{l+1-n}}{(\beta_1-\beta_2)(n-l)!} \left(e^{-\beta_1} \sum_{k=0}^{n} \binom{n}{k} (-\alpha/\beta_1)^{n-k} \cdot R(\alpha, \beta_1 | p) \right. \\
&\qquad \left. - e^{-\beta_2} \sum_{k=0}^{n} \binom{n}{k} (-\alpha/\beta_2)^{n-k} \cdot R(\alpha, \beta_2 | p) \right)
\end{aligned} \tag{5.10}$$

where $p = k - l - 1$ and $R(\cdot, \cdot|p)$ is the integral expression of (5.7) in Appendix A.

Bibliography

[1] S. Catreux, P. F. Driessen, and L. J. Greenstein, "Simulation results for an interference-limited multiple-input multiple-output cellular system," *IEEE Commun. Lett.*, vol. 4, no. 11, pp. 334-336, 2000.

[2] S. Ye and R. S. Blum, "Optimized signaling for MIMO interference systems with feedback," *IEEE Trans. Signal Process.*, vol. 51, no. 11, pp. 2839-2848, 2003.

[3] M. Sadek, A. Tarighat, and A. H. Sayed, "A leakage-based precoding scheme for downlink multi-user MIMO channels," *IEEE Trans. Wireless Commun.*, vol. 6, no. 5, pp. 1711-1721, 2007.

[4] R. S. Blum, "MIMO capacity with interference," *IEEE J. Select. Areas Commun.*, vol. 21, no. 5, pp. 793-801, 2003.

[5] B. O. Lee, H. W. Je, O. -S. Shin, and K. B. Lee, "A novel uplink MIMO transmission scheme in a multicell environment," *IEEE Trans. Wireless Commun.*, vol. 8, no. 10, pp. 4981-4987, 2009.

[6] K. N. Lau, "Analytical framework for multiuser uplink MIMO spacetime scheduling design with convex utility functions," *IEEE Trans. Wireless Commun.*, vol. 3, no. 5, pp. 1832-1843, 2004.

[7] Y. Hara, L. Brunel, and K. Oshima, "Uplink spatial scheduling with adaptive transmit beamforming in multiuser MIMO systems," in *Proceedings of the IEEE*

International Symposium on Personal, Indoor & Mobile Radio Communications, Helsinki, Finland, 11-14 Sep. 2006.

[8] S. Serbetli and A. Yener, "Beamforming and scheduling strategies for time slotted multiuser MIMO systems," in *Proceedings of the Asilomar Conference on Signals, Systems & Computers*, Pacific Grove, CA, USA, 7-10 Nov. 2004.

[9] Leakage-based precoding for CoMP in LTE-A, 3GPP R1-090028, 2009.

[10] Coordinated multi-point operation for LTE physical layer aspects (release 11), 3GPP TR 36.819, V11.1.0, 2011.

[11] G. Dimic and N. D. Sidiropoulos, "On downlink beamforming with greedy user selection: performance analysis and a simple new algorithm," *IEEE Trans. Signal Process.*, vol. 53, no. 10, pp. 3857-3868, 2005.

[12] P. Patcharamaneepakorn, A. Doufexi, and S. Armour, "Reduced complexity joint user and receive antenna selection algorithms for SLNR-based precoding in MU-MIMO systems," in *Proceedings of the IEEE Vehicular Technology Conference*, Yokohama, Japan, 6-9 May 2012.

[13] T. Yoo and A. Goldsmith, "On the optimality of multiantenna broadcast scheduling using zero-forcing beamforming," *IEEE J. Select. Areas Commun.*, vol. 24, no. 3, pp. 528-541, 2006.

[14] Further consideration on enhanced SRS for CoMP/non-CoMP user group, 3GPP R1-095087, 2009.

[15] D. Gesbert, D. Hanly, H. Huang, S. Shamai, O. Simeone, and W. Yu, "Multi-cell MIMO cooperative networks: A new look at interference," *IEEE J. Select. Areas Commun.*, vol. 28, no. 9, pp. 1380-1408, 2010.

[16] Z.-Q. Luo and S. Zhang, "Dynamic spectrum management: Complexity and duality," *IEEE J. Select. Topics Signal Process.*, vol. 2, no. 1, pp. 57-73, 2008.

[17] E. G. Larsson and E. A. Jorsweick, "Competition versus cooperation on the MISO interference channel," *IEEE J. Select. Areas Commun.*, vol. 27, no. 7, pp. 1059-1069, 2008.

[18] E. A. Jorswieck, E. G. Larsson, and D. Danev, "Complete characterization of the Pareto boundary for the MISO interference channel," *IEEE Trans. Signal Process.*, vol. 56, no. 10, pp. 5292-5296, 2008.

[19] R. Zhang and S. Cui, "Cooperative interference management with MISO beamforming," *IEEE Trans. Signal Process.*, vol. 58, no. 10, pp. 5454-5462, 2010.

[20] X. Shang, B. Chen, and H. Poor, "Multiuser MISO interference channels with single-user detection: Optimality of of beamforming and the achievable rate region," *IEEE Trans. Inf. Theory*, vol. 57, no. 7, pp. 4255-4273, 2011.

[21] J. Lindblom, E. Karipidis, and E. G. Larsson, "Selfishness and altruism on the MISO interference channel: the case of partial transmit CSI," *IEEE Commun. Lett.*, vol. 13, no. 9, pp. 667-669, 2009.

[22] R. Mochaourab and E. A. Jorswieck, "Exchange economy in two-user multiple-input single-output interference channels," *IEEE J. Select. Topics Signal Process.*, vol. 6, no. 2, pp. 151-164, 2012.

[23] J. Lindblom and E. Karipidis, "Cooperative beamforming for the MISO interference channel," in *Proceedings of the IEEE European Wireless Conference*, Lucca, Italy, 12-15 Apr. 2010.

[24] P. Cao, E. A. Jorsweick, and S. Shi, "Pareto Boundary of the rate region for single-stream MIMO interference channels: linear transceiver design," *IEEE Trans. Signal Process.*, vol. 61, no. 20, pp. 4907-4922, 2013.

[25] J. Qiu, R. Zhang, Z -Q. Luo, and S. Cui, "Optimal distributed Beamforming for MISO interference channels," *IEEE Trans. Signal Process.*, vol. 59, no. 11, pp. 5638-5643, 2011.

[26] R. Zakhour and D. Gesbert, "Coordination on the MISO interference channel using the virtual SINR framework," in *Proceedings of the Internatioanl ITG Workshop on Smart Antennas*, Berlin, Germany, 16-19 Feb. 2009.

[27] R. Zakhour and D. Gesbert, "Distributed multicell-MISO precoding using the layered virtual SINR framework," *IEEE Trans. Wireless Commun.*, vol. 9, no. 8, pp. 2444-2448, 2010.

[28] R. Bhagavatula and R. Heath, "Adaptive limited feedback for sum rate maximizing beamforming in cooperative multicell systems," *IEEE Trans. Signal Process.*, vol. 59, no. 2, pp. 800-811, 2011.

[29] M. A. Vazquez, A. Perez-Neira, and M. A. Lagunas, "Generalized eigenvector for decentralized transmit beamforming in the MISO interference channel," *IEEE Trans. Signal Process.*, vol. 61, no. 4, pp. 878-882, 2013.

[30] N. Jindal, J. G. Andrews, and S. Weber, "Rethinking MIMO for wireless networks: Linear throughput increases with multiple receive antennas," in *Proceedings of the IEEE International Conference on Communications*, Dresden, Germany, 14-18 Jun. 2009.

[31] A. Osseiran, *et al*., "Scenarios for 5G mobile and wireless communications: The vision of the METIS Project," *IEEE Commun. Mag.*, vol. 52, no. 5, pp. 26-35, 2014.

[32] Scenarios and requirements for small cell enhancements for E-URTA and E-UTRAN (Release 12), 3GPP, TR 36.932, v12.0.0, 2012.

[33] N. Bhushan, *et al.*, "Network densification: The dominant theme for wireless evolution into 5G," *IEEE Commun. Mag.*, vol. 52, no. 2, pp. 82-89, 2014.

[34] M. K. Karakayali, G. J. Foschini, and R. A. Valenzuela, "Network coordination for spectrally efficient communications in cellular systems," *IEEE Commun. Mag.*, vol. 13, no. 4, pp. 56-61, 2006.

[35] X. You,*et al.* , "Cooperative distributed antenna systems for mobile communications [Coordinated and Distributed MIMO]," *IEEE Trans. Wireless Commun.*, vol. 17, no. 3, pp. 35-43, 2010.

[36] M. Rahman and H.Yanikomeroglu, "Enhancing cell-edge performance: a downlink dynamic interference avoidance scheme with inter-cell coordination," *IEEE Trans. Wireless Commun.*, vol. 9, no. 4, pp. 1414-1425, 2010.

[37] A. Papadoginnis, D. Gesbert, and E. Hardouin, "A dynamic clustering approach in wireless networks with multi-cell cooperative processing," in *Proceedings of the IEEE International Conference on Communications*, Beijing, China, 19-23 May 2008.

[38] J. Zhang, R. Chen, J. G. Andrews, A. Ghosh, and R. W. Heath, "Networked MIMO with clustered linear precoding," *IEEE Trans. Wireless Commun.*, vol. 8, no. 4, pp. 1910-1921, 2009.

[39] J. M. Moon and D. H. Cho, "Inter-cluster interference management based on cell-clustering in network MIMO systems," in *Proceedings of the IEEE Vehicular Technology Conference*, Budapest, Hungary, 15-18 May 2011.

[40] M. Hong, R. Sun, H. Baligh, and Z. Q. Luo, "Joint base station clustering and beamforming design for partial coordinated transmission in heterogeneous networks," *IEEE J. Select. Areas Commun.*, vol. 31, no. 2, pp. 226-240, 2013.

[41] P. Baracca, F. Boccardi, and N. Benvenuto, "A dynamic clustering algorithm for downlink CoMP systems with multiple antenna UEs," *EURASIP Journal on Wireless Communications and Networking*, vol. 124, Jan. 2013.

[42] M. Yoon, M.-S. Kim, and C. Lee, "A dynamic cell clustering algorithm for maximization of coordination gain in uplink coordinated system," *IEEE Trans. Vehicular Tech.*, vol. 65, no. 3, pp. 1752-1760, 2016.

[43] H. Zhang, H. Liu, C. Jiang, X. Chu, A. Nallanathan, and X. Wen, "A practical semidynamic clustering scheme using affinity propagation in cooperative picocells," *IEEE Trans. Vehicular Tech.*, vol. 64, no. 9, pp. 4372-4377, 2015.

[44] B. J. Frey and D. Dueck, "Clustering by passing messages between data points," *Science*, vol. 315, no. 5814, pp. 972-976, 2007.

초 록

셀 간 간섭 문제는 셀룰러 시스템의 성능을 제한하는 중요한 요소이며, 특히 셀 간 주파수 재사용율이 높을 때 더 큰 성능 제한이 발생한다. 다중셀 다중 안테나 기술은 이러한 셀 간 간섭의 영향으로 성능 저하가 발생하게 된다. 본 논문에서는 다중셀 다중 안테나 환경에서 셀 간 간섭을 제어하는 기법을 제안한다.

본 논문의 전반부에서는 다운링크 다중셀 다중안테나 시스템을 위한 사용자 선택 기법을 제안한다. 다운링크 사용자 선택문제는 인접셀의 사용자 선택의 영향을 받기 때문에 문제의 복잡도가 크다. 따라서 기존의 사용자 선택 기법은 인접셀의 간섭을 고려하지 않고, 기지국과 사용자의 채널정보만을 이용하여 선택 하였으나, 이는 간섭을 고려하지 않았기 때문에 성능을 크게 개선 하지 못했다. 그리고 모든 사용자 조합을 비교하여 전송률이 가장 좋은 사용자를 선택하는 기법이 제안되었으나 간섭을 고려 하기 때문에 성능은 크게 개선되었지만, 모든 사용자 조합을 비교하기 때문에 복잡도가 매우 커서 실제 환경에 적용하기 어려운 단점이 있다. 제안하는 기법은 전송률을 최대화 할 수 있는 사용자를 순차적으로 선택하는 기법이다. 구체적으로, 전송률 증가를 나타내는 메트릭을 제안하고, 이를 이용하여 기존의 사용자 선택 기법보다 복잡도를 상당히 줄 일 수 있는 사용자 선택 기법을 제안한다.

본 논문의 중반부에서는 반복적인 동작이 필요하지 않은 협력 빔포밍 기법을 제안한다. 빔포밍은 신호채널의 세기를 고려하면서 동시에 간섭채널을 줄여야 한다. 기존에 제안된 빔포밍은 반복적인 동작을 통해 Pareto optimality 를 찾는 빔포밍 기법이다. 하지만 이 기법은 셀의 수가 많아 지면 복잡도가 기하급수적으로 증가하여 현실의 통신시스템에 적용하기가 어렵다는 단점이 있다. 이러한 단점을 보완하기

위해 신호대발생간섭잡음비(SGINR)을 제안하고 이를 최대화 하는 빔포밍 기법이 제안되었다. 이는 반복적인 동작이 필요하지 않다는 장점이 있지만, 최대화 하는 신호대발생간섭잡음비 메트릭은 전송률 메트릭과 차이가 있고, 또한 높은 신호대잡음비(SINR)을 가정하기 때문에 셀 경계의 사용자들의 성능을 개선 할 수 없다는 단점이 있다. 이러한 단점을 개선하기 위해 제안하는 빔포밍 기법은 반복적인 동작이 없이 간섭채널을 줄이며 동시에 신호 채널 세기의 균형을 유지하는 빔포밍 기법이다. 또한 전송률 메트릭 자체를 최대화 하는 빔포밍 기법으로 셀 경계의 사용자들의 전송률도 개선 할 수 있다. 제안하는 기법에서는 평균 전송률의 분석을 통해 global selfishness 라는 것을 정의하고, 이를 이용하여 각 기지국이 스스로 협력하는 빔포밍 벡터를 만들 수 있게 한다. 본 기법은 기존의 비포밍 기법과는 다르게 2-cell 시스템뿐 아니라 3-cell 시스템에도 수학적인 확장과 적용이 가능하다.

본 논문의 후반부에서는 Coordinated multi-point (CoMP) 시스템을 위한 메시지 전달 기반의 셀 클러스터링 기법을 제안한다. 5G 통신 시스템에서는 동시에 많은 수의 기지국이 통신을 할 것으로 기대되고 있으며, 이러한 고밀도 셀룰러 환경에 기존의 중앙집중적 셀 클러스터링 방식은 적용 할 수 가 없다. 따라서 본 연구에서는 메시지 전달을 통한 분산형 셀 클러스터링 기법을 제안한다. 제안하는 셀 클러스터링 기법은 분산적 동작으로 동작하여 복잡도를 줄일 수 있고, 이는 고밀도 환경에 적용하기에 적합한 기술이다. 또한 기존의 클러스터링 기법과 다르게 CoMP Joint Processing 과 CoMP Coordinated Beamforming/Coordinated Scheduling 에 모두 적용 가능한 기술이다.

주요어: 셀 간 간섭, 다중셀 다중안테나 시스템, 사용자 선택, 빔포밍, 셀 클러스터링
학번: 2011-30217